Cell Reports
Medicine

Article

Contact-dependent inhibition of HIV-1 replication in *ex vivo* human tonsil cultures by polymorphonuclear neutrophils

Graphical abstract

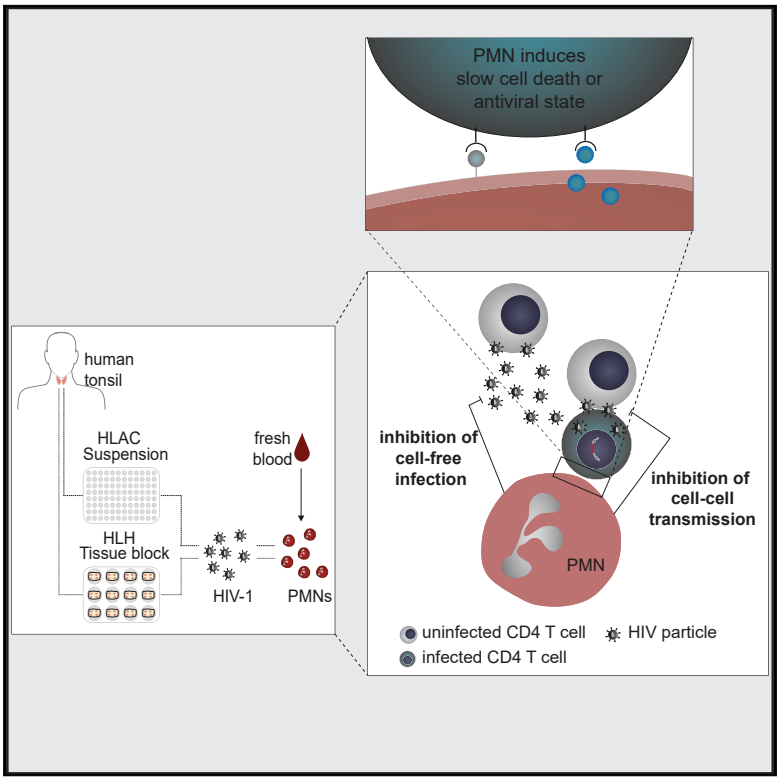

Highlights

- PMNs blunt HIV-1 spread and CD4 T cell depletion in HIV-infected human tonsils
- Suppression of HIV-1 replication by PMNs requires cell-cell contacts
- PMNs do not affect HIV via effector functions such as NETosis or degranulation
- PMNs exert unconventional antiviral activity

Authors

Tatjana Reif, Gerhard Dyckhoff, Ralph Hohenberger, ..., Eicke Latz, Bettina Stolp, Oliver T. Fackler

Correspondence

oliver.fackler@med.uni-heidelberg.de

In brief

Polymorphonuclear neutrophils (PMNs) exert anti-microbial activity, but whether they affect HIV-1 replication in primary target cells had not been assessed. Reif et al. report that addition of PMNs to HIV-infected human tonsils potently suppresses HIV-1 spread and virus-induced depletion of CD4 T cells via an unconventional mechanism mediated by cell-cell contacts.

Reif et al., 2021, Cell Reports Medicine 2, 100317
June 15, 2021
https://doi.org/10.1016/j.xcrm.2021.100317

CellPress

Cell Reports Medicine

CellPress
OPEN ACCESS

Article

Contact-dependent inhibition of HIV-1 replication in *ex vivo* human tonsil cultures by polymorphonuclear neutrophils

Tatjana Reif,[1] Gerhard Dyckhoff,[2] Ralph Hohenberger,[2] Carl-Christian Kolbe,[3] Henning Gruell,[4,5] Florian Klein,[4,5] Eicke Latz,[3] Bettina Stolp,[1] and Oliver T. Fackler[1,6,7,*]

[1]Department of Infectious Diseases, Integrative Virology, University Hospital Heidelberg, 69120 Heidelberg, Germany
[2]Department of Otorhinolaryngology, Head and Neck Surgery, University Hospital Heidelberg, 69120 Heidelberg, Germany
[3]Institute of Innate Immunity, Department of Innate Immunity and Metaflammation, University Hospital Bonn, 53127 Bonn, Germany
[4]Laboratory of Experimental Immunology, Institute of Virology, Faculty of Medicine and University Hospital Cologne, University of Cologne, 50931 Cologne, Germany
[5]German Center for Infection Research (DZIF), Partner Site Bonn-Cologne, 50931 Cologne, Germany
[6]German Center for Infection Research (DZIF), Partner Site Heidelberg, 69120 Heidelberg, Germany
[7]Lead contact
*Correspondence: oliver.fackler@med.uni-heidelberg.de
https://doi.org/10.1016/j.xcrm.2021.100317

SUMMARY

Polymorphonuclear neutrophils (PMNs), the most abundant white blood cells, are recruited rapidly to sites of infection to exert potent anti-microbial activity. Information regarding their role in infection with human immunodeficiency virus (HIV) is limited. Here we report that addition of PMNs to HIV-infected cultures of human tonsil tissue or peripheral blood mononuclear cells causes immediate and long-lasting suppression of HIV-1 spread and virus-induced depletion of CD4 T cells. This inhibition of HIV-1 spread strictly requires PMN contact with infected cells and is not mediated by soluble factors. 2-Photon (2PM) imaging visualized contacts of PMNs with HIV-1-infected CD4 T cells in tonsil tissue that do not result in lysis or uptake of infected cells. The anti-HIV activity of PMNs also does not involve degranulation, formation of neutrophil extracellular traps, or integrin-dependent cell communication. These results reveal that PMNs efficiently blunt HIV-1 replication in primary target cells and tissue by an unconventional mechanism.

INTRODUCTION

Invading pathogens face a wide range of innate and adaptive immune responses that need to be bypassed or counteracted for efficient spread in the new host. In this tug-of-war between pathogen and host, polymorphonuclear neutrophils (PMNs), the most abundant human white blood cells, are considered a first line of host defense. High numbers of PMNs are recruited rapidly to sites of infection or sterile injury, where they can survive for as long as 7 days to exert potent anti-microbial activities.[1-3] Pathogen elimination by PMNs can occur by a wide array of PMN effector functions that include degranulation of secretory granules with anti-microbial content such as α-defensins and myeloperoxidase (MPO), production of reactive oxygen species (ROS), release of neutrophil extracellular traps (NETs), phagocytosis, or trogocytosis of pathogens, cancer cells, and virus-infected cells.[4-8] In addition, PMNs can indirectly affect pathogen survival by regulation of innate and adaptive immune responses; e.g., by affecting production of interferon-γ by other immune cells.[2] Which of these mechanisms are triggered varies between pathogens, and most studies focus on effects of PMNs on bacteria and fungi. Among viruses, PMNs are best studied in the context of respiratory infections such as influenza A virus (IAV) and severe acute respiratory syndrome coronavirus 2 (SARS-CoV-2), where inflammation in infected lungs is associated with massive PMN recruitment and activation.[9-11] For IAV, an important role of PMNs in controlling virus spread in mouse models has been established,[12,13] and the ability of PMNs to modulate the antiviral adaptive immune response is well documented.[14-17] Moreover, neutrophil-to-lymphocyte ratios are used increasingly as predictive markers for the clinical course of respiratory virus infection.[18-20] A series of *in vitro* studies also reported direct antiviral activity of PMN secretory granule components or NETs toward additional viruses, including herpes simplex virus (HSV) 1 and 2, cytomegalovirus, vesicular stomatitis virus, respiratory syncytial virus, and vaccinia virus,[21-26] but whether PMNs play a physiologically relevant role in controlling these infections remains unclear.

This scenario particularly applies to human immunodeficiency virus type 1 (HIV-1), the causative agent of AIDS; host responses to acute HIV-1 infection are thought to be dominated by innate immune-sensing events and cell-intrinsic antiviral factors (restriction factors).[27-29] Although it is well established that PMN numbers and function, including adhesion and chemotaxis, are impaired in

individuals with HIV,[30-34] the antiviral role of PMNs is not well studied. The few reports addressing whether PMNs can affect HIV-1 infection or spread observed that artificial activation of PMNs by phorbol 12-myristate 13-acetate (PMA) interfered with HIV-1 replication in a T cell line and defined production of MPO and ROS triggered by PMN activation as the inhibitory components.[35] Moreover, incubation of PMNs with high concentrations of cell-free HIV-1 virions has been shown to induce NET production in a Toll-like receptor (TLR)7/8-dependent manner *ex vivo*.[36-38] Although these studies indicated that PMNs may be able to exert anti-HIV activity, they did not assess whether PMNs impair HIV-1 replication in physiologically relevant target cells and tissue, where virus spread occurs predominately via cell-associated transmission and not cell-free virus particles.[39-41] We therefore set out to study the effects of PMNs on HIV-1 replication in *ex vivo* cultures of human tonsil tissue and peripheral blood mononuclear cells (PBMCs). We find that PMNs exert immediate and potent anti-HIV-1 activity that requires direct cell-cell contact but is not mediated by any of the classic PMN effector functions described so far.

RESULTS

PMNs reduce HIV-1 titers and CD4 T cell depletion in an *ex vivo* tonsil histoculture and PBMCs

The goal of this study was to define whether PMNs exert antiviral activity toward HIV-1 in the context of multiple rounds of virus infection in primary human target tissue. We therefore used *ex vivo* cultures of human tonsil tissue as a model system that allows following HIV-1 spread and associated CD4 T cell depletion in a natural HIV-1 target tissue explant without the need for experimental cell activation, thus serving as an approximation of HIV infection of lymphoid tissue.[42-46] Tonsil tissue removed by routine tonsillectomy from HIV-negative donors was processed to suspension cultures (human lymphoid aggregate culture [HLAC]) or tissue blocks (human lymphoid histoculture [HLH])[42-45] and infected with HIV-1_{NL4-3} SF2 Nef, a well-characterized, laboratory-adapted X4 tropic HIV-1 variant encoding for the *nef* gene of HIV-1_{SF2}.[46,47] Viral titers were monitored over approximately 2 weeks by determining the reverse transcriptase (RT) activity in the cell culture supernatant using the SYBR (2-{2-[(3-Dimethylamino-propyl)-propylamino]-1-phenyl-1*H*-chinolin-4-ylidenmethyl}-3-methyl-benzothiazol-3-ium-Kation) Green-based product enhanced reverse transcriptase assay (SG-PERT). The extent of CD4 T cell depletion was analyzed by flow cytometry 12–14 dpi (Figure 1A). Under these conditions, HIV-1 spread efficiently in HLACs, as indicated by a robust increase of RT activity in the cell culture supernatant over time (Figure 1B, control [ctrl]), which was suppressed efficiently when the HIV-1 fusion inhibitor enfuvirtide (+T20) was added to HIV-1-infected samples 24 h post infection (pi). HLACs contained a complex array of cell types, including CD4 and CD8 T lymphocytes, B cells, monocytes, macrophages, and dendritic cells,[43,48] but did not contain detectable amounts of PMNs (data not shown). To test the effect of PMNs on HIV-1 spread, we added 1×10^6 freshly isolated PMNs to infected cultures 24 h pi. Interestingly, addition of PMNs to HIV-1-infected cultures exerted an immediate negative effect on virus spread because RT activity in the supernatant did not increase further over time but declined in a manner comparable with T20-treated cultures (Figure 1B, +PMNs). These results suggest that the addition of PMNs prevents infection of additional target cells but does not suppress residual production of virus particles from cells that were infected in the initial round of infection in the absence of PMNs. Relative CD4 T cell depletion, calculated as the ratio of $CD3^+/CD8^-$ (CD4 T cells) versus $CD3^+/CD8^+$ (CD8 T cells), was only observed in cultures infected with HIV-1 in the absence of PMNs, whereas addition of PMNs abrogated CD4 T cell depletion (Figures 1C and 1D). Importantly, addition of PMNs did not affect the viability or abundance of CD4+ T cells in uninfected HLACs (Figure 1C). This interference with HIV-1 spread by PMNs was observed reproducibly using HLACs and PMNs from several donors; comparing viral load by plotting the area under the curve (AUC) of virus replication over 14 days, as shown in Figure 1B, revealed a more than 100-fold reduction in HIV-1 replication in the presence of PMNs (Figure 1E). This reduction in virus replication by PMNs was associated with a significant 4-fold decrease in HIV-1-induced CD4 T cell depletion (Figure 1F). Importantly, PMNs also potently suppressed HIV-1 replication in HLH tissue blocks, indicating that this antiviral activity of PMNs is also exerted in the context of infection of HIV target tissue with physiological architecture (Figures 1G and S1A–S1D). Because, in these experiments, PMNs were added to HLAC or HLH cultures from heterologous donors, the observed antiviral effect might have involved nonspecific reactions between cells from different donors. Once we had the opportunity to obtain matched HLAC and PMNs from the same donor and observed that inhibition of HIV-1 replication in these cultures by autologous PMNs was at least as potent as by heterologous PMNs (Figure 1H). Moreover, HIV-1 replication in PBMCs was also inhibited by PMNs independent of whether they were of autologous or heterologous origin (Figures 1I, S1E, and S1F). PMNs thus bear antiviral activity that can suppress HIV-1 replication and virus-induced CD4 T cell depletion in *ex vivo* lymphoid explant and PBMC cultures.

PMN-mediated inhibition of HIV-1 replication is independent of the viral strain and time point of PMN addition but dependent on the PMN:HLAC ratio

Because all experiments described above were conducted with the same CXCR4 using a lab-adapted HIV-1 strain, we next tested whether PMNs exert antiviral activity against R5 tropic and primary HIV-1 strains. HLACs were infected with an R5 tropic variant of HIV-$1_{NL4.3}$ (R5 HIV-1) or the R5 tropic primary transmitted founder virus (T/FV) HIV-1_{CH058} and cultured in the presence of 1×10^6 PMNs for 13 days (Figures 2A, 2B and S2A). Similar to infection with X4 HIV-1 (Figure 1B), PMNs immediately caused a decline of virus replication of both HIV-1 variants, indicating that PMN-mediated inhibition of HIV-1 replication is independent of cell tropism and not restricted to lab-adapted strains. An immediate reduction of viral titers was also observed when PMNs were added 4 or 5 days after HIV-1 infection (Figures 2C and S2B). Addition of PMN to infected cultures can thus also blunt virus spread at later time points. In line with previous reports,[3] PMNs were viable for more than 72 h after addition to HLAC cultures, and the presence of HIV did not affect PMN survival (Figure 2D). Notably, HIV-1 replication did not

CellPress
OPEN ACCESS

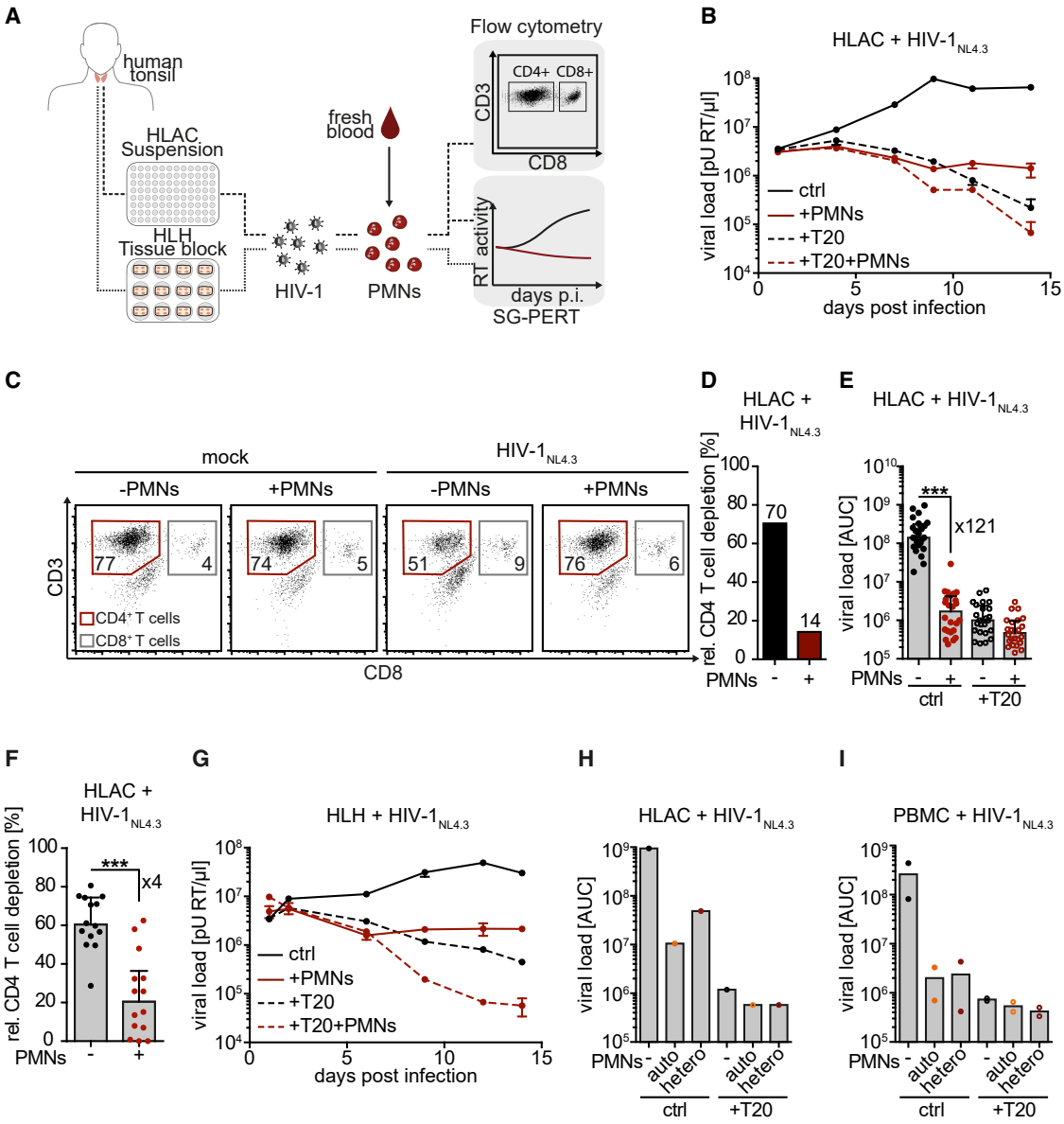

Figure 1. PMNs inhibit HIV-1 replication in HLACs and HLH

(A) Schematic of the experimental setup. HLACs and HLH were prepared from human tonsils, infected with HIV-1, and cultured in the presence (red) or absence (black) of 1 × 10^6 PMNs for 12–14 days. Cell culture supernatant was harvested every 2–3 days, and viral load was analyzed by SG-PERT.

(B) Representative replication curves of HIV-1-infected HLACs ± T20 in the presence or absence of PMNs. Data points are mean values + SD of triplicate infections of cells from the same donor.

(C) Representative flow cytometry dot plots of the cells analyzed in (B), stained for CD3 and CD8 at 14 dpi, followed by analysis of CD4 T cell depletion. Numbers indicate the percentage of cells of the total living cell population in the respective gate.

(D) CD4 T cell depletion of the experiment shown in (C). The ratio of CD4 ($CD3^+CD8^-$) and CD8 ($CD3^+CD8^+$) T cells was calculated, and CD4 T cell depletion was determined relative to the respective mock samples, which were arbitrarily set to 0.

(E) HIV-1 replication, depicted as the area under the curve (AUC) of 23 independent experiments performed in triplicates (mean + SD).

(F) CD4 T cell depletion in HLACs from 14 donors, analyzed at 12–14 days post infection (dpi) as shown in (D). Shown are mean values of experiments performed in triplicates + SD.

(G) Representative replication curves of HIV-1-infected HLHs ± T20 in the presence or absence of PMNs. Data points are mean values + SD of duplicates from one well containing four HLH blocks of the same donor.

(H and I) HLACs from one donor (H) or activated PBMCs from two donors (I) were infected with X4 HIV-1 and cultured in the presence of 1 × 10^6 autologous (orange) or heterologous (red) PMNs or in the absence (black) of PMNs for additional 13 (HLACs) or 14 (PBMCs) days.

Gray bars with errors in (E) and (F) indicate the median + interquartile range of all experiments and the fold reduction, respectively. Data points are mean values + SD of triplicate infections of cells from the same donor. Statistical significance was assessed by Mann-Whitney *U* test (*p < 0.05, **p < 0.01, ***p < 0.0001). See also Figure S1.

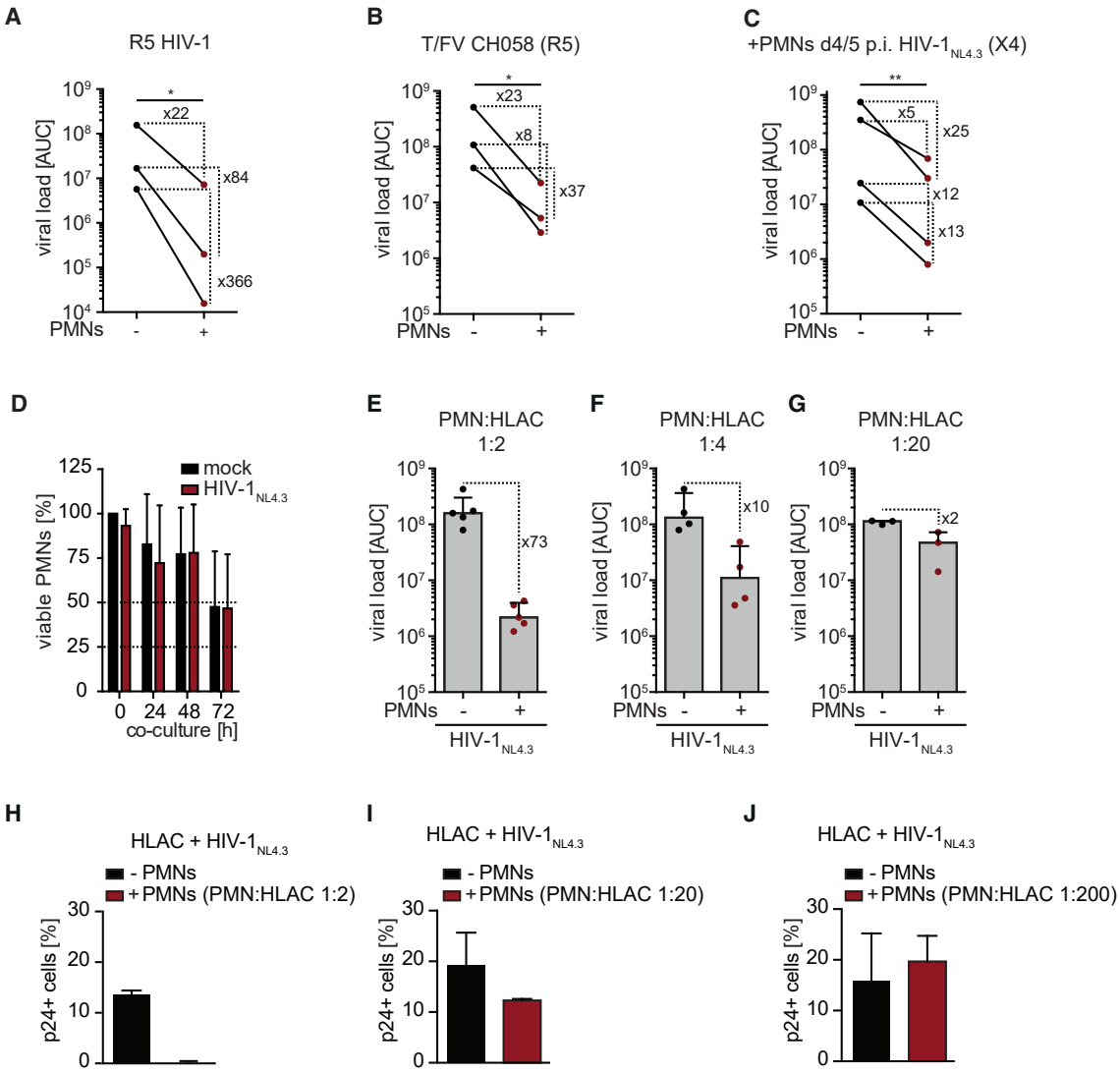

Figure 2. PMN-mediated inhibition of HIV-1 replication is independent of the viral strain and time point of PMN addition but depends on the PMN:HLAC ratio

Cell culture supernatants for viral load determination by SG-PERT were harvested every 2–3 days.

(A and B) HLACs were infected with (A) R5 HIV-1 or (B) the primary HIV-1 isolate T/FV CH058 and cultured in the presence or absence of 1 × 10^6 PMNs for 14 days. Presented are mean AUC values of HIV-1 replication over 14 days from independent experiments performed in triplicates, with each individual data point representing cells from 3 distinct donors.

(C) HLACs infected with X4 HIV-1 were cultured in the presence or absence of 1 × 10^6 PMNs added on day 4/5 pi for 14 days. Data points are mean AUC values of a 7-day period starting from the time point of PMN addition of independent experiments performed in triplicates, with each individual data point representing cells from 4 distinct donors.

(D) HLACs were infected with X4 HIV-1 or left uninfected (mock) and cultured in the presence of 1 × 10^6 PMNs for 72 h. At 0 h, 24 h, 48 h, and 72 h, cells were stained with the viability dye V450, the PMN marker CD66b, and the T cell marker CD3 and analyzed by flow cytometry. Shown is the percentage of viable PMNs normalized to the mock sample at 0 h (set to 100%). Depicted are mean values + SD from 4 independent experiments performed in triplicates.

(E–G) HLACs were infected with X4 HIV-1 and cultured in the presence or absence of 1 × 10^6 (1:2, E), 5 × 10^5 (1:4, F), or 1 × 10^5 (1:20, G) PMNs for 14 days. Shown are mean AUC values of HIV-1 replication of 3–5 experiments performed in triplicates. Gray bars with errors and numbers indicate the median + interquartile range or the fold change of all experiments, respectively. Data points are mean values + SD of triplicate infections of cells from the same donor.

(H–J) HLACs of the same donor were infected with X4 HIV-1, cultured in the presence or absence of 1 × 10^6 (1:2, H), 1 × 10^5 (1:20, I), or 1 × 10^4 (1:200, J) PMNs, and the amount of productively infected cells was determined by intracellular flow cytometry for p24Gag 6 days post infection. Shown are mean values + SD of triplicate infections.

See also Figure S2.

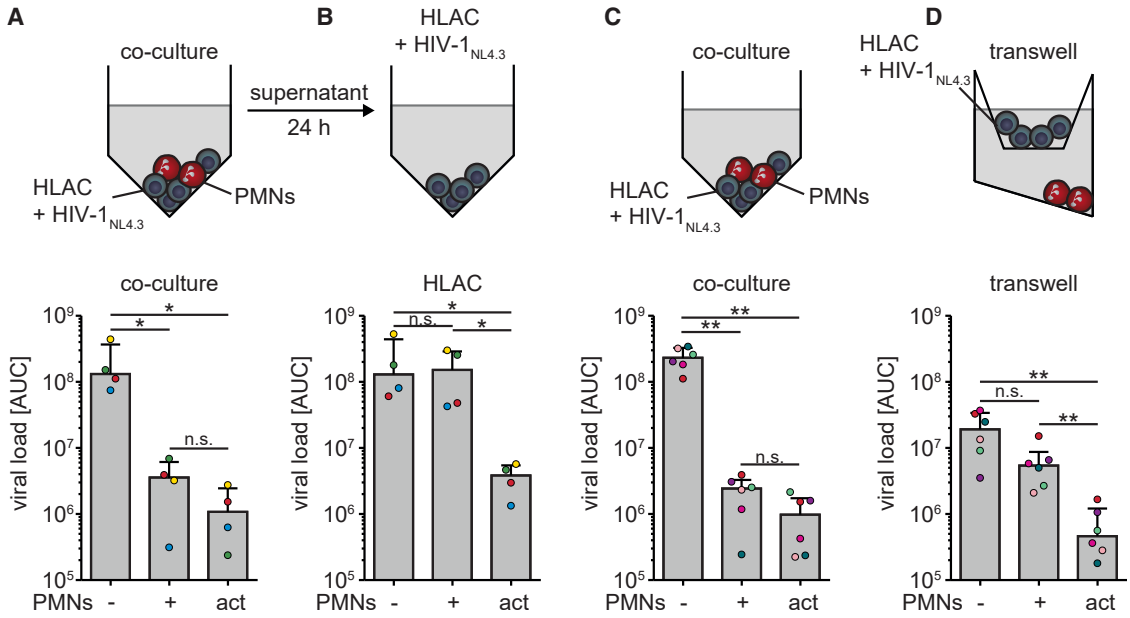

Figure 3. PMN-mediated inhibition of HIV-1 replication depends on cell-cell contacts

(A–D) HLACs were infected with X4 HIV-1 and cultured for 13 days in the presence or absence of 1 × 10^6 native or PMA pre-activated PMNs (A and C), treated with the supernatant from (A) (B), or spatially separated from native or PMA pre-activated PMNs by a membrane with 1-μm pore size (D). Cell culture supernatants were harvested every 2–3 days for determination of viral load by SG-PERT and are presented as AUC values for the integrated viral load over the duration of the entire experiment for HLAC-PMN co-cultures of 4 (A and B) or 6 (C and D) HLAC donors.

(A) Standard HLAC-PMN co-culture.

(B) Supernatant of HLAC-PMN co-cultures in (A) was transferred 24 h after PMN addition to infected HLACs (tissue from the same donors as in A).

(C) Standard HLAC-PMN co-culture.

(D) HLAC-PMN co-culture with tissue from the same donors as in (C) but with physical separation of infected HLAC and PMNs.

Note that viral titers of the control co-culture experiment (C) are higher than titers of the Transwell experiment (D) because the volume of a standard 96-well V-bottom is smaller than the overall volume of the Transwell system. Gray bars with errors indicate the median + interquartile range of all experiments. Data points are mean values + SD of triplicate infections of cells from the same donor. Associated datasets from individual donors are color coded. Each statistical significance was assessed by Mann-Whitney *U* test (not significant [ns], $p > 0.05$; *$p < 0.05$; **$p < 0.01$). See also Figure S3.

resume over 14 days of replication (Figures 1B, 1G, and S1A–S1D) and, thus, long after the amounts of viable PMNs had declined. Physiologically, PMNs are recruited in high numbers to sites of infection and sterile injury to ensure potent anti-microbial effects.[49] Such marked infiltration may be reflected by the 1:2 ratio of PMNs to infected HLACs used in most of our experiments, which resulted in potent inhibition of X4 HIV-1 replication (>70-fold inhibition in this experimental series; Figure 2E). Interestingly, PMN-mediated inhibition was already reduced to 10-fold when a 1:4 ratio was used (Figure 2F), and adding PMNs at a 1:20 ratio almost completely abrogated the antiviral activity of PMNs (2-fold inhibition) (Figure 2G). Notably, this reduction of virus production induced by addition of PMNs was paralleled by a marked reduction in the number of p24-positive cells in HLAC cultures when high but not low amounts of PMNs were added (Figures 2H–2J). Potent and long-lasting inhibition of HIV-1 replication by PMNs is thus achieved during the short lifespan of PMNs in these cultures but requires a high abundance of PMNs. These results suggest that the immediate antiviral effect of PMNs results in irreversible and quantitative elimination or inactivation of infected cells in these cultures. Because this effect was observed with X4 and R5 tropic HIV-1, X4 tropic HIV-1 can also infect macrophages in HLACs, and CD4 T cells are the predominant target of HIV-1 infection in tonsil tissue,[50] we focused on X4 tropic HIV for the subsequent studies.

PMN-mediated inhibition of HIV-1 replication depends on cell-cell contacts

Next we wanted to gain insight into the PMN effector function(s) involved in inhibition of HIV-1 replication. Because a main PMN effector mechanism involves release of granular content into the phagolysosome or the extracellular space by degranulation, we first tested whether secretion of anti-viral effector molecules into the supernatant is essential for inhibition of HIV-1 replication. To this end, we co-cultured X4 HIV-1-infected HLACs and PMNs for 24 h (Figure 3A) and transferred the supernatant to a monoculture of HIV-1-infected HLACs (Figure 3B). As a positive control, PMNs pre-activated with PMA (act) were used because it has been shown that the supernatant of artificially pre-activated PMNs is sufficient to reduce HIV-1 replication.[35] In these co-cultures, PMNs and pre-activated PMNs inhibited HIV-1 replication to a similar extent (Figure 3A). Importantly, transfer of the supernatant of co-cultures with native PMNs did not reduce HIV-1 replication in infected HLACs, whereas the supernatant of co-cultures with pre-activated PMNs caused a decline of HIV-1 replication

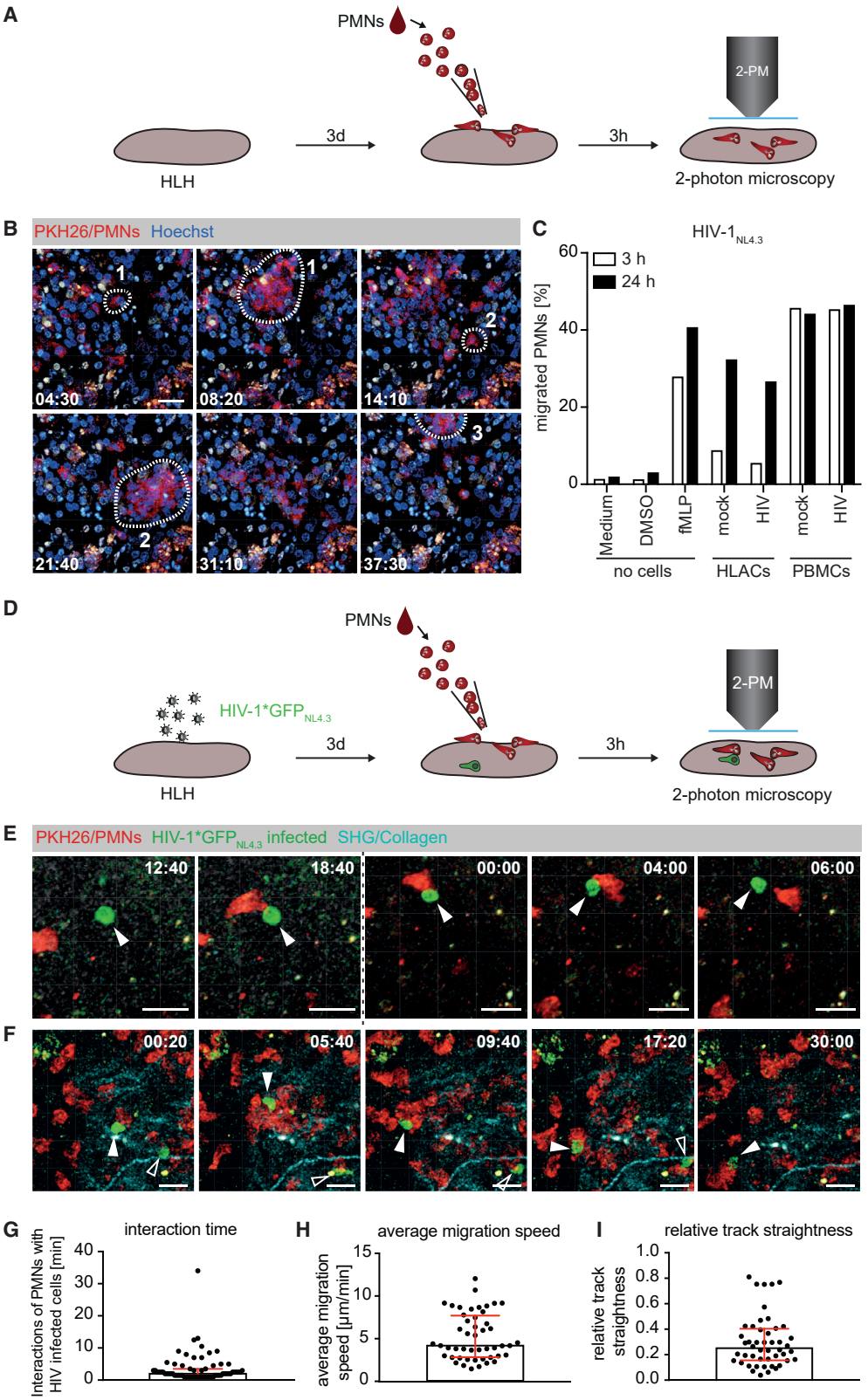

(legend on next page)

that was almost as potent as in the direct co-culture (Figure 3B). This effect was independent of the duration of the HLAC-PMN co-cultures because comparable results were obtained with supernatants taken from co-cultures after 3 h (Figure S3B), 6 h (Figure S3C), 48 h (Figure S3D), or 72 h (Figure S3E).

These results suggest that release of antiviral compounds into the cell culture supernatant was not sufficient to explain the anti-HIV activity of native PMNs. To specifically address whether this inhibitory effect required direct contact between PMNs and HLACs, we next compared direct co-cultures allowing cell-cell contacts (Figure 3C) with cultures in Transwell chambers in which PMNs and HLACs were physically separated by a membrane with 1-μm pore size, which prevented PMN migration and direct contact (Figure 3D). Although PMNs efficiently inhibited HIV-1 replication in direct co-cultures, this antiviral activity was almost completely abrogated when the two cell populations were separated by a Transwell porous membrane. In contrast, and consistent with release of a soluble antiviral compound, pre-activated PMNs reduced HIV-1 replication to a similar extent in both experimental settings. These results reveal that native PMNs exert their anti-HIV activity in a manner that strictly depends on direct cell contact with infected HLACs and is fundamentally distinct from the action of artificially pre-activated PMNs.

Visualization of contacts between HIV-1-infected CD4 T cells and PMNs in HLH

To gain insight into the anti-HIV activity of PMNs, we next sought to visualize the behavior of PMNs in HLH blocks (Figure 4A) and their interactions with HIV-1 infected CD4 T cells (Figure 4D) by 2-photon microscopy (2PM). PMNs efficiently swarm to sites of infection with multiple pathogens or upon sterile injury.[51] Interestingly, addition of PKH26-labeled PMNs to uninfected HLH (Figures 4A and 4B) revealed immediate infiltration of PMNs into the tissue and subsequent formation of transient swarms (Figure 4B; Video S1). PMNs were also attracted to non-infected HLACs and PBMCs in a Transwell migration assay with an efficacy that was comparable with the very potent chemotactic stimulant N-formylmethionine-leucyl-phenylalanine (fMLP) (Figure 4C). In line with this observation and consistent with activation of PMNs, the PMN surface markers CD66b, CD63, and CD64 were upregulated and CD16 was downregulated when added to HLACs, and these changes occurred independent of HIV-1 infection (Figures S4A–S4D). Such activation was also detectable at the level of cytokine production, where addition of PMNs to HLACs triggered production of typical PMN cytokines such as MCP-1 or HGF, but, again, this cytokine response was comparable between mock and HIV-infected cultures and, thus, elicited by PMN interactions with HLAC components independent of HIV (Figure S4E). Production of interferon α or γ was not observed in these cultures, which may reflect that only moderate amounts of these cytokines were produced that were below the level of detection in our assay. HIV infection is thus neither required for basal PMN activation nor their efficient infiltration into cultures of human lymphoid tissue or PBMCs.

To determine whether and how PMNs interact physically with HIV-1-infected CD4 T cells, HLHs were infected with HIV-1*GFP, which expresses GFP in productively infected cells.[52] 3 dpi, PMNs were seeded onto HIV-1*GFP-infected tissue blocks to allow their infiltration and analyzed by 2PM for up to 3 h (Figure 4D). This analysis allowed us to detect several events where HIV-1-infected cells underwent contacts with PMNs. One type of interaction consisted of rather transient contacts (less than 10 min) of single PMNs with infected cells (Figure 4E; Video S2). At later time points, dissolving PMN swarms were followed, and a single HIV-1 infected cell was observed to remain in prolonged contact with a single PMN (>30 min; Figure 4F; Video S3). Before engaging in these transient or prolonged contacts, PMNs did not display a particular chemotactic behavior, and no swarming toward infected cells was observed. The encounter between PMNs and HIV-infected CD4 T cells also did not have appreciable immediate consequences for both cell types involved because cell disintegration or engulfment was not detected during the observation period. Manual tracking of interacting cells revealed the majority of interactions between PMNs and HIV infected cells to be transient (Figure 4G; median interaction time, 2 ± 4.7 min) with repetitive interactions of various PMNs with a single HIV-infected cell occurring frequently. Long-lasting interactions were observed only rarely (longest continuous interaction, 34 min). Tracking of HIV-infected cells irrespective of PMN interactions revealed considerable migratory capacity of HIV-infected CD4 T cells in HLH. Migration speed (Figures 4H; 4.22 ± 2.73 μm/min median speed)

Figure 4. Visualization of PMN CD4 T cell contacts in HIV-1-infected tonsil tissue blocks by 2-photon microscopy (2PM)

(A) Schematic overview of the experimental setup for analysis of uninfected HLH. 1 × 10^6 PKH26-labeled PMNs were added on top of the HLH. Hoechst was added to the culture medium to visualize the tissue environment, and the HLH was imaged with 2PM for 40 min. Images were taken every 20 s.

(B) Still images of a representative 2PM video (Video S1), showing the motility of PMNs in uninfected HLH. PMN swarms are encircled by dotted lines. Numbers indicate the order of appearance. Scale bars, 20 μm.

(C) 3 × 10^4 PKH67-labeled PMNs were subjected to a Transwell chemotaxis assay toward medium, DMSO, 100 nM fMLP, or mock- or HIV-1-infected HLACs or PBMCs. Cells were allowed to migrate for 3 h or 24 h at 37°C, resuspended in PBS + precision counting beads, and quantified by flow cytometry. Depicted is the mean percentage of migrated PMNs after 3 h (white) and 24 h (black) of one experiment performed in duplicates.

(D) Schematic overview of the experimental setup for HIV-infected HLHs. HLHs were infected with 5 × 10^4 infectious units of HIV-1*GFP. 3 dpi, 1 × 10^6 PKH26-labeled PMNs were added on top of the tissue blocks.

(E and F) HLHs were imaged directly after PMN addition (E) or 3 h after PMN addition (F) by 2PM for 30 min. Images were taken every 20 s. Shown are still images of the videos, with white arrowheads pointing to infected cells. In (E), the last 3 images are from a second video that was started immediately after the first video stopped (images 1 and 2). Shown are PMNs (red), nuclei (blue), HIV-1-infected cells (green), and second harmonic generation (SHG)/collagen (cyan). Scale bars, 20 μm. See also Videos S1, S2, and S3.

(G–I) HIV-1-infected cells were tracked manually using InViewR (Arivis) for interactions with PMNs (G), migration speed (H), and track straightness (I). Each data point represents an individual interaction or track, with the bar indicating median with interquartile range.

See also Figure S4.

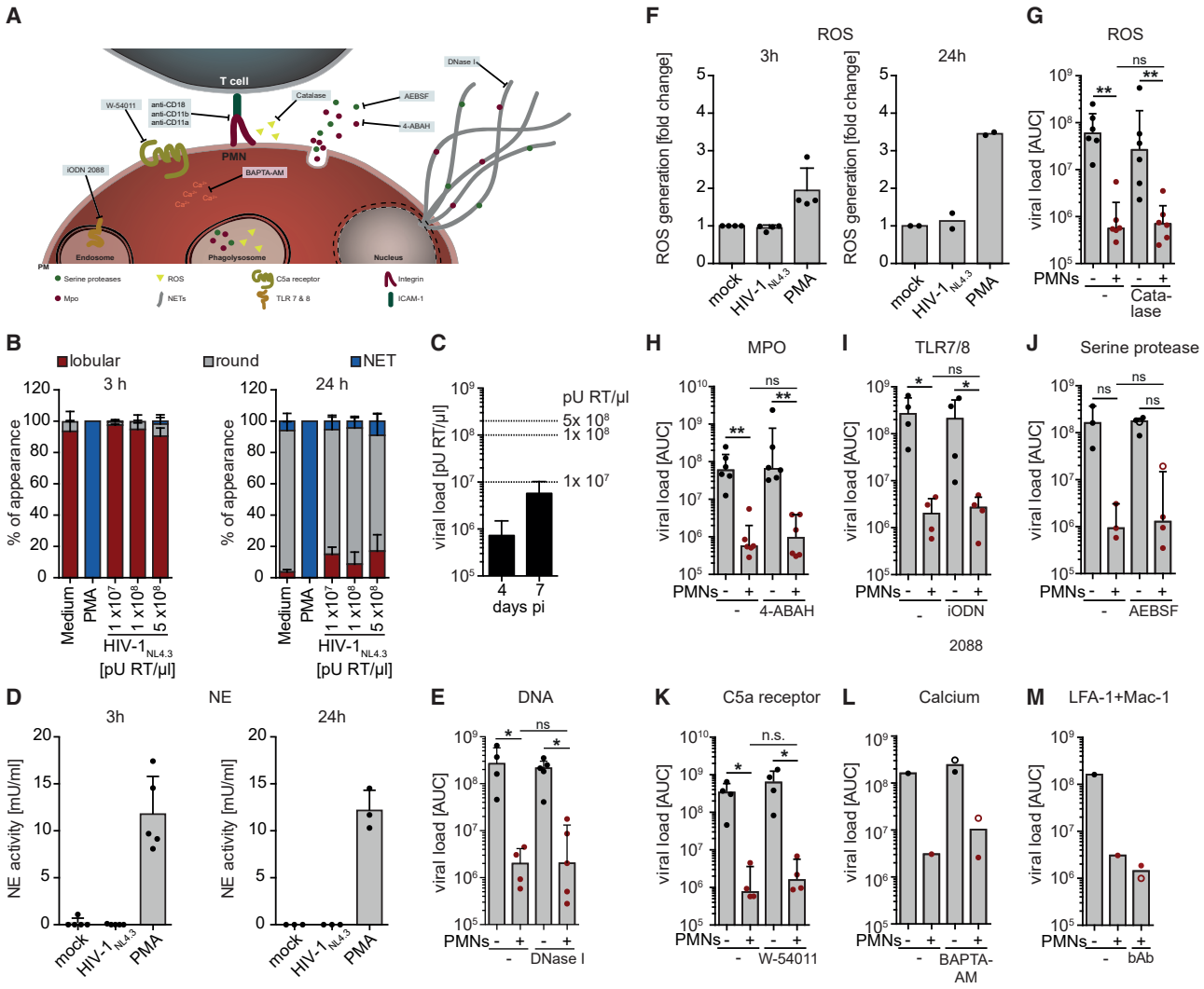

Figure 5. The reduction of HIV-1 titers is independent of classic PMN effector functions

(A) Schematic overview of the different PMN effector functions and drugs or blocking antibodies used.

(B) Quantification of NET formation by PMNs incubated with HIV-1 particles. PMNs were co-cultured with medium, 100 nM PMA, or different amounts of viral particles on fibronectin-coated cover glasses for 3 h and 24 h. Samples were stained with anti-MPO antibody and Hoechst. 5 random images (see Figure S5A for images) were taken per condition and time point, and NET-forming cells were counted manually. In PMA-treated samples, differentiation between NET-forming cells and normal PMNs was not possible because of the overall coverage of the selected areas with NETs. NET formation in these samples was set as an approximate value of 100%. For the other samples, PMNs were categorized as lobular nucleus (red), round nucleus (gray), and NET forming (blue). Depicted are mean values + SD of 4 and 3 independent experiments for 3 h and 24 h, respectively.

(C) HLACs were infected with X4 HIV-1, and supernatant for determination of the viral load by SG-PERT was harvested on days 4 and 7 pi. Depicted are mean values + SD of 8 independent experiments performed in triplicates. Dotted lines indicate the number of viral particles used in (B).

(D) Production of NE. HLACs were infected with X4 HIV-1 or left uninfected (mock) and cultured in the presence of 1×10^6 PMNs for 3 h and 24 h. As a positive control, 20 nM PMA was added to the mock culture. At the indicated time point, NE activity was determined ($n_{3h} = 5$, $n_{24h} = 3$). Shown are mean values of experiments performed in duplicates or triplicates.

(E) 5 U/mL DNase I was added to X4 HIV-1-infected HLACs cultured with or without 1×10^6 PMNs. Each symbol designates the AUC of HIV-1 replication of 4–5 independent experiments performed in triplicates, hostogram bars indicate mean values + SD.

(F) ROS production; experiment as in (D) but analyzed for ROS production by flow cytometry. Shown are mean values + SD of experiments performed in triplicates ($n_{3h} = 4$, $n_{24h} = 2$) relative to mock samples (set to 1).

(G–M) Experiment as in (E) but using the following agents to affect PMN activity: (G) 1,000 U/mL catalase, (H) 100 µM 4-ABAH (n = 6), (I) 1 µM iODN 2088 (n = 4), (J) 50 µM AEBSF (n = 3), (K) 300 µM W054011 (n = 4), (L) 10 µM BAPTA-AM (n = 2), and (M) 100 µg/mL blocking antibody against CD18, CD11a, and CD11b (n = 1 or 2). Cells were treated for 30 min before addition to X4 HIV-1 infected HLACs, and experiments were performed in the presence of the inhibitors. Shown are mean values + SD of experiments performed in duplicates or triplicates.

(legend continued on next page)

and directionality (Figure 4I; median track straightness, 0.26 ± 0.2) of these HIV-1-infected cells were comparable with migration of HIV-1-infected cells in 3D collagen matrices.[39] Our 2PM analysis thus allowed us to visualize physical contacts between PMNs and HIV-1-infected cells that do not result in an immediately appreciable effect on the infected cell.

Inhibition of HIV-1 replication by PMNs is independent of classic PMN effector functions

Because imaging showed formation of contacts between PMNs and HIV-infected CD4 T cells in HLH but did not provide indications about the molecular events that mediate inhibition of HIV-1 spread, we next assessed the involvement of classic anti-microbial effector functions. To this end, we monitored production of anti-microbial components in infected HLAC-PMN co-cultures and assessed the effect of specific inhibitors targeting individual PMN activities on HIV-1 spread (Figure 5A; see Figure S5H for cell viability at the inhibitor concentrations used). We first tested whether PMNs release NETs in this experimental system, as described to occur in response to high amounts of HIV 1 viral particles and to reduce HIV infectivity.[36] We therefore considered the possibility that HIV-1 particles released in the cell culture supernatant or the local high concentrations of HIV-1 particles at cell-cell contacts formed to transmit the virus from infected donor to uninfected target cells (virological synapse)[40,53-55] might trigger a similar response and contribute to the anti-HIV-1 activity in HLACs. Hence, we incubated PMNs with various amounts of HIV particles (between 1×10^7–5×10^8 pU RT/μL) and stained these samples for DNA and MPO to detect NETs (Figures 5B and S5A). Although the positive control PMA rapidly induced NET formation in virtually all PMNs, incubation with HIV particles did not result in significantly higher NET production relative to the medium control (Figures 5B, 3 h). Although longer incubation (Figure 5B, 24 h) resulted in a change of the typical lobular shape of PMN nuclei in control and HIV-treated samples, significant formation of NETs was not observed. Importantly, the lowest amount of HIV particles used in these experiments corresponded to the amount detected in infected HLAC at peak viremia, and NET production was not observed even when 50-fold more virions were used (Figure 5C). Neutrophil elastase (NE), a marker for NET release associated with extracellular NET fibers,[36,56] was also produced by PMNs only after PMA treatment but not in co-cultures with HIV-infected HLAC (Figure 5D). In line with this absence of NET production, adding DNase I to HLAC-PMN co-cultures at the time of PMN addition at a concentration that degraded PMA-induced extracellular DNA fibers did not reverse the inhibition of PMNs on HIV-1 replication (Figures 5E and S5B). Production of ROS, which was involved in HIV-1 particle-dependent NET formation,[36] was also not triggered in HIV-infected co-cultures (Figure 5F), and the ROS inhibitor catalase (Figure 5G), which neutralized ROS produced at the concentration used (Figure S5C), did not impair the anti-HIV activity of PMNs in infected HLACs. Inhibition of MPO, an enzyme stored in azurophilic granules that is crucial for inhibition of HIV-1 replication by PMA pre-activated PMNs incubated with viral particles as well as NET formation in response to HIV-1 particles,[35,36] with 4-aminobenzoic acid hydrazide (4-ABAH) did not reverse inhibition of HIV-1 replication by PMNs (Figures 5H and S5D). Finally, NET release by PMNs in response to contact with HIV particles has been reported to be triggered via TLR7/8 signaling.[36] However, inhibition of TLR7/8 by inhibitory oligodeoxynucleotide (iODN) 2088 did not impair the anti-HIV activity of PMNs in infected HLACs (Figure 5I). These results imply that inhibition of HIV-1 replication in HLACs by PMNs does not involve formation of NETs or the activity of NET-associated anti-microbial PMN components and suggest that the previously described induction of NETosis[36,37] may result from incubation of PMNs with nonphysiologically high amounts of HIV-1 particles.

We therefore next assessed the relevance of additional PMN effector molecules or signaling pathways. This included inhibition of serine protease activity involved in PMN trogocytosis required for killing *T. vaginalis*[6] with 4-(2-aminoethyl) benzenesulfonylfluoride (AEBSF) (Figure 5J). In addition, because it has been shown to be involved in PMN chemotaxis and degranulation,[57-59] we interfered with C5a using the C5a receptor agonist W-54011 (Figure 5K). Another study showed antibody-mediated trogoptosis of cancer cells by PMNs involving release of Ca^{2+},[7] which was inhibited by the calcium chelator BAPTA-AM (Figure 5L). Finally, PMNs depend on cell surface lymphocyte function- associated antigen 1 (LFA-1) (CD18/CD11a) and Mac-1 (complement receptor 3 [CR3], CD18/ CD11b) to facilitate PMN arrest on endothelial cells, and Mac-1 has also been shown to be involved in conjugate formation between PMNs and T cells;[7,60-63] thus, we incubated PMNs with blocking antibodies against CD18, CD11b, and CD11a before addition to HLACs (Figure 5M; see Figures S5E–S5G for antibody blocking efficiency). Remarkably, none of these treatments impaired the anti-HIV activity of PMNs in infected HLACs. These results suggest that inhibition of HIV-1 replication in HLACs by PMNs is exerted by a still to be identified, non-conventional effector function.

DISCUSSION

Because PMNs constitute the first line of defense against many pathogenic microorganisms but their role in HIV-1 spread in physiological target cells had not yet been evaluated, the goal of this study was to assess the effects of PMNs on HIV-1 spread in primary human CD4 T cells. Our analyses revealed that, in *ex vivo* cultures of human tonsil tissue or PBMCs, PMNs can exert potent anti-HIV activity that rapidly suppresses virus replication. This activity was observed with lab-adapted and primary HIV variants irrespective of their co-receptor use and was exerted by PMNs from heterologous donors as well as from the one autologous donor we were able to test. Interference with HIV replication is thus a general intrinsic property of PMNs. These findings suggest that PMNs are a relevant arm of the innate immune response against HIV-1 infection.

Open circles indicate mean values of data points of experiments in which the cells of the control experiment could not be analyzed because of cell death. Gray bars with errors indicate the mean + SD of all experiments. Data points are mean values + SD of triplicate infections of cells from the same donor. Statistical significance was assessed by Mann-Whitney *U* test (*p < 0.05, **p < 0.01). See also Figure S5.

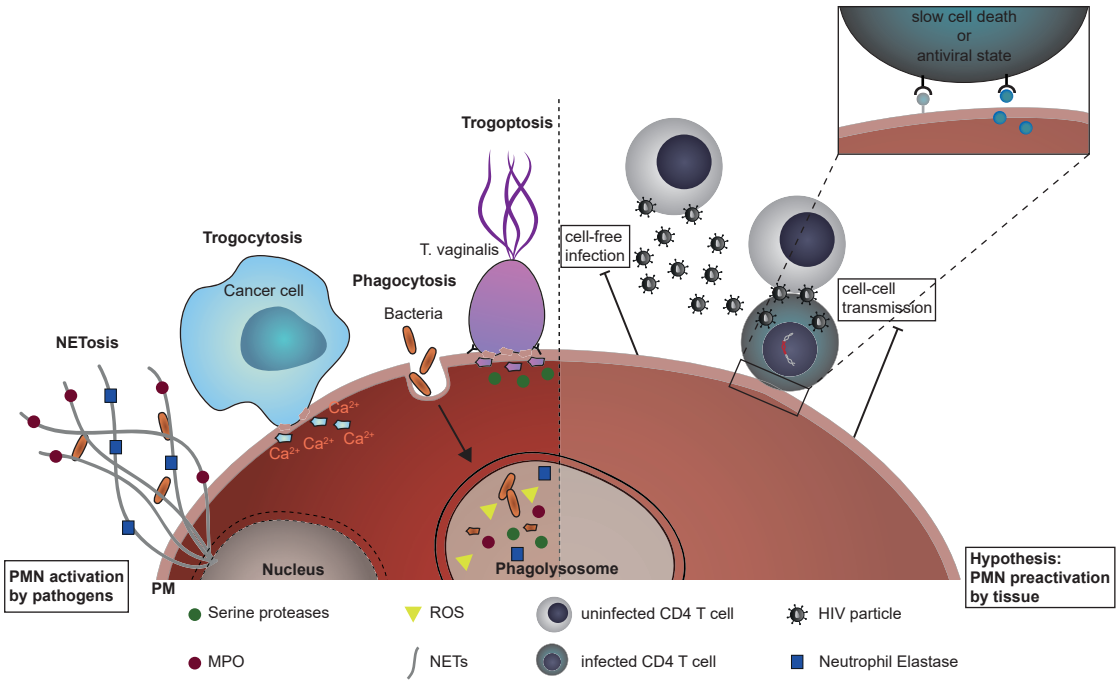

Figure 6. Schematic model of contact-dependent inhibition of HIV-1 replication by PMNs

Depicted are established PMN effector functions (NETosis, trogocytosis, phagocytosis, and trogoptosis) described to act against bacteria, parasites, and cancer cells (left half). On the right, the characteristics of contact-dependent inhibition of HIV-1 replication in tonsil tissue are shown. See text for details.

Using artificial PMN activation or nonphysiologically high amounts of virus particles, previous studies have revealed the potential of PMN effector functions, such as release of MPO or NET, to interfere with HIV-1 spread in cell lines.[35,36] In contrast, characterization of the anti-HIV-1 activity in our primary cell systems revealed that inhibition of HIV-1 spread did not involve these effector functions because (1) neither NET formation nor PMN activation resulting in release of ROS was induced in HIV-1-infected cultures, and (2) inhibitors of NET formation or ROS and MPO activity failed to suppress the anti-HIV activity of PMNs. The antiviral activity of PMNs we observed in HIV-1-infected HLACs is thus fundamentally mechanistically distinct from previously described effects of PMNs on HIV-1 infection and occurs at physiological levels of HIV-1 replication in primary human explant culture. Moreover, inhibitors of other anti-microbial effector functions, including serine protease activity for elimination of the parasite *T. vaginalis* by trogoptosis, C5a and Mac-1 interactions that drive complement activation, and cell interaction and calcium release required for trogoptosis of cancer cells, did not impair the ability of PMNs to suppress HIV-1 spread (Figure 6, left panel). These results suggest that PMNs act on HIV-1 by an unconventional and still to be identified molecular mechanism.

Although the molecular details of this unconventional inhibition of HIV-1 spread by PMNs remain to be identified, our analysis characterized a series of properties of this anti-HIV activity (Figure 6, right panel). A central feature of this process is its strict dependence on direct cell contacts of PMNs with HIV-1-infected CD4 T cells, which likely explains why high PMN ratios are required for efficient suppression of HIV-1 spread. Unlike, e.g., fungal infections, HIV-infected cells did not seem to potently chemoattract PMNs, and interactions with HIV infected cells did not trigger PMN activation, as judged by surface exposure of established PMN activation markers, induction of cytokine release, and triggering of classical PMN effector functions. Rather, uninfected tonsil tissue or PBMCs were sufficient to attract PMNs and trigger expression of activation markers on and cytokines by PMNs. We thus hypothesize that contact with uninfected tissue induces a state of pre-activation that is functionally distinct from full-blown activation by, e.g., PMA but may prime PMNs to exert their anti-HIV activity. The ability of HIV-1 particles to bind to PMNs[64] may contribute to the observed reduction in HIV-1 replication. However, because the supernatant of HIV-1-infected cultures challenged with PMNs did not display anti-HIV activity, physical separation of HIV-infected HLAC and PMNs abrogated the negative effect of PMNs on HIV-1 spread, and PMNs reduced the amounts of productively infected cells, the main effect of PMNs must be directly on HIV-1-infected cells. This could involve targeted and confined secretion of anti-HIV components at cell-cell contacts or induction of signaling cascades by receptor engagement or targeted release of components at cell-cell contacts that trigger antiviral programs. Future studies will focus on identifying transcriptional changes that could account for the inhibition of HIV-1 replication.

Our attempts to visualize the interaction of PMNs with HIV-1-infected CD4 T cells in infected tonsil tissue readily revealed

such cell-cell interactions. However, these cell-cell contacts (1) did not display formation of typical synapse-like structures that mediate, e.g., lysis of target cells by cytotoxic T or natural killer (NK) cells[65,66] and (2) did not lead to targeted cell uptake or lysis within the observation period. These results are most consistent with a mechanism that triggers antiviral signaling in infected CD4 T cells upon cell-cell contact without the need for stable and polarized interaction in the form of a synapse. Of note, addition of PMNs to HIV-1-infected cultures not only suppressed production of new HIV particles but also potently reduced the amounts of virus-producing (p24-positive) cells. This suggests that antiviral signaling induced by PMNs limits viral gene expression and/or long-term survival of HIV-1 infected CD4 T cells. Both mechanisms would reduce production of new viral progeny and limit HIV-1 spread by cell-free and cell-associated transmission modes and would be consistent with the observed blunting of virus spread upon PMN addition. Because the suppression of HIV-1 replication lasted far beyond the lifespan of PMNs in the culture, we currently favor the hypothesis that PMNs exert a negative effect on the survival of infected CD4 T cells that is not observed immediately after initiation of cell-cell contacts but after the time frame we were able to capture by our imaging analyses. Although inhibition of HIV-1 spread by PMNs was often highly efficient and comparable with the effect of the entry inhibitor T20, residual low-level virus production persisted over time despite addition of PMNs in some experiments. This may indicate donor variability in the sensitivity to PMN inhibition or the ability of the virus to circumvent inactivation by PMNs. Future research, which will include transcriptional profiling of infected cells and PMNs, will focus on defining the molecular mechanisms that allow PMNs to recognize HIV-infected CD4 T cells and inactivate virus production of these cells.

Several observations in individuals with HIV suggest that PMNs may indeed contribute to control of HIV-1 spread; low PMN counts in high-risk groups are associated with an elevated likelihood to acquire HIV-1 infection, including mother-to-child transmission;[30,31] PMN function is impaired in individuals with chronic HIV-1;[32,33] and PMNs have been described to infiltrate lymph nodes in HIV-infected individuals.[34] Because murine PMNs also exerted anti-HIV activity when added to infected human tonsil cultures (data not shown), we tested the effect of PMN depletion on HIV-1 replication in humanized mice (data not shown). These experiments did not reveal an increase in HIV-1 replication upon PMN depletion. To compare animals with individual HIV replication kinetics, PMN depletion had to be induced after robust virus titers had been established at peak viremia, which limited the possibility to observe an additional increase in virus titer. Nevertheless, these results indicate that PMNs may be involved in limiting acute HIV infection at transmission sites rather than systemic virus replication in individuals with chronic HIV. In support of this hypothesis, PMNs are present at HIV transmission sites such as vaginal mucosae (e.g., HSV-2),[67,68] and enhanced PMN chemotaxis is associated with low rates of HIV-1 transmission.[69]

Here we describe that, in our *ex vivo* HLAC model, PMNs exert potent inhibition of HIV-1 spread in cultures of primary human target cells and tissue that is not mediated by classical PMN effector functions but via an unconventional mechanism. These results suggest PMNs to be a previously overlooked arm in the innate arsenal of host defense to HIV infection and possibly other viruses.

Limitations of the study

Although this study reveals potent anti-HIV activity of PMNs added to infected HLACs, the underlying mechanism and relevance to AIDS pathogenesis remain to be established. Our results with specific pharmacological inhibitors suggest that PMNs suppress HIV-1 spread by an unconventional mechanism. Although these treatments were titrated carefully to occur at the highest non-cytotoxic concentration, and controls for the effectiveness of the drugs were included when possible, we cannot fully exclude that some of these known effectors contribute to PMN-mediated suppression of HIV-1 replication. In addition, the imaging approaches used to visualize the effect of PMNs on HIV-1-infected cells in HLH blocks (1) did not allow fluorescent labeling of uninfected CD4 T cells or other cell types during 2PM imaging, and (2) quantification of cell-cell interactions on fixed HLH tissue sections by immune histology was hampered by bleaching of the GFP signal of HIV-infected cells during fixation. Finally, the HLA cultures used here do not reflect the cell composition and activity at mucosal portals of HIV entry and do not recapitulate all aspects of lymphoid tissue *in vivo*, and our *in vivo* experiment could not be conducted via mucosal virus transmission. Future studies will thus require testing of the effect of PMN depletion on HIV-1 spread in mucosal explants and natural transmission animal models and visualizing the interactions of HIV-1-infected cells and PMNs in this context.

STAR★METHODS

Detailed methods are provided in the online version of this paper and include the following:

- KEY RESOURCE TABLE
- RESOURCE AVAILABILITY
  - Lead contact
  - Materials availability
  - Data and code availability
- EXPERIMENTAL MODEL AND SUBJECT DETAILS
  - Human lymphoid aggregate culture (HLAC), human lymphoid histoculture (HLH) and peripheral blood mononuclear cells (PBMC)
  - Isolation of polymorphonuclear neutrophils (PMN)
  - Cell culture
- METHOD DETAILS
  - Virus production, infectivity measurements, infection assays and CD4 T cell depletion
  - Pharmacological inhibition of PMN effector functions
  - 1μm transwell assay
  - 3μm transwell chemotaxis assay
  - Supernatant swap experiment
  - Neutrophil elastase (NE) activity
  - Neutrophil MPO activity assay kit
  - Immunofluorescence

- Reactive oxygen species (ROS) production
- 2-photon microscopy (2PM) of HLHs

● QUANTIFICATION AND STATISTICAL ANALYSIS

SUPPLEMENTAL INFORMATION

Supplemental information can be found online at https://doi.org/10.1016/j.xcrm.2021.100317.

ACKNOWLEDGMENTS

This study was supported by DFG (German Research Foundation) Projektnummer 240245660, SFB 1129, and TRR83 project 15 (to O.T.F.). We are grateful to the IDIP imaging facility at the CIID and its support by the Deutsche Zentrum für Infektionsforschung (DZIF). The authors gratefully acknowledge the data storage service SDS@hd, supported by the Ministry of Science, Research and the Arts Baden-Württemberg (MWK) and the DFG through grants INST 35/1314-1 FUGG and INST 35/1503-1 FUGG. We are deeply indebted to the numerous anonymous donors that made this study possible and to Steffen Geis, Marlis Gerigk, Isabel Barreto-Miranda, Dina Khalid, Stefan Windhaber, and Lars Maurer for drawing blood.

AUTHOR CONTRIBUTIONS

Conceptualization, O.T.F.; methodology, T.R. and B.S.; investigation, T.R., B.S., H.G., and C.C.K.; writing – original draft, O.T.F., T.R., and B.S.; writing – review & editing, O.T.F., T.R., B.S., G.D., and H.G.; funding acquisition, O.T.F.; resources, E.L., F.K., R.H., and G.D.; supervision, O.T.F., B.S., E.L., and F.K.

DECLARATION OF INTERESTS

The authors declare no competing interests.

Received: July 24, 2020
Revised: March 2, 2021
Accepted: May 20, 2021
Published: June 15, 2021

REFERENCES

1. Kolaczkowska, E., and Kubes, P. (2013). Neutrophil recruitment and function in health and inflammation. Nat. Rev. Immunol. *13*, 159–175.
2. Ley, K., Hoffman, H.M., Kubes, P., Cassatella, M.A., Zychlinsky, A., Hedrick, C.C., and Catz, S.D. (2018). Neutrophils: New insights and open questions. Sci. Immunol. *3*, eaat4579.
3. Pillay, J., den Braber, I., Vrisekoop, N., Kwast, L.M., de Boer, R.J., Borghans, J.A., Tesselaar, K., and Koenderman, L. (2010). In vivo labeling with 2H2O reveals a human neutrophil lifespan of 5.4 days. Blood *116*, 625–627.
4. Rudkin, F.M., Bain, J.M., Walls, C., Lewis, L.E., Gow, N.A., and Erwig, L.P. (2013). Altered dynamics of Candida albicans phagocytosis by macrophages and PMNs when both phagocyte subsets are present. MBio *4*, e00810–e00813.
5. Lu, T., Porter, A.R., Kennedy, A.D., Kobayashi, S.D., and DeLeo, F.R. (2014). Phagocytosis and killing of Staphylococcus aureus by human neutrophils. J. Innate Immun. *6*, 639–649.
6. Mercer, F., Ng, S.H., Brown, T.M., Boatman, G., and Johnson, P.J. (2018). Neutrophils kill the parasite Trichomonas vaginalis using trogocytosis. PLoS Biol. *16*, e2003885.
7. Matlung, H.L., Babes, L., Zhao, X.W., van Houdt, M., Treffers, L.W., van Rees, D.J., Franke, K., Schornagel, K., Verkuijlen, P., Janssen, H., et al. (2018). Neutrophils Kill Antibody-Opsonized Cancer Cells by Trogoptosis. Cell Rep. *23*, 3946–3959.e6.
8. Van Strijp, J.A., Van Kessel, K.P., van der Tol, M.E., Fluit, A.C., Snippe, H., and Verhoef, J. (1989). Phagocytosis of herpes simplex virus by human granulocytes and monocytes. Arch. Virol. *104*, 287–298.
9. Tomar, B., Anders, H.J., Desai, J., and Mulay, S.R. (2020). Neutrophils and Neutrophil Extracellular Traps Drive Necroinflammation in COVID-19. Cells *9*, 1383.
10. Mozzini, C., and Girelli, D. (2020). The role of Neutrophil Extracellular Traps in Covid-19: Only an hypothesis or a potential new field of research? Thromb. Res. *191*, 26–27.
11. Camp, J.V., and Jonsson, C.B. (2017). A Role for Neutrophils in Viral Respiratory Disease. Front. Immunol. *8*, 550.
12. Tate, M.D., Brooks, A.G., and Reading, P.C. (2008). The role of neutrophils in the upper and lower respiratory tract during influenza virus infection of mice. Respir. Res. *9*, 57.
13. Tumpey, T.M., García-Sastre, A., Taubenberger, J.K., Palese, P., Swayne, D.E., Pantin-Jackwood, M.J., Schultz-Cherry, S., Solórzano, A., Van Rooijen, N., Katz, J.M., and Basler, C.F. (2005). Pathogenicity of influenza viruses with genes from the 1918 pandemic virus: functional roles of alveolar macrophages and neutrophils in limiting virus replication and mortality in mice. J. Virol. *79*, 14933–14944.
14. Mócsai, A. (2013). Diverse novel functions of neutrophils in immunity, inflammation, and beyond. J. Exp. Med. *210*, 1283–1299.
15. Galani, I.E., and Andreakos, E. (2015). Neutrophils in viral infections: Current concepts and caveats. J. Leukoc. Biol. *98*, 557–564.
16. Naumenko, V., Turk, M., Jenne, C.N., and Kim, S.J. (2018). Neutrophils in viral infection. Cell Tissue Res. *371*, 505–516.
17. Mantovani, A., Cassatella, M.A., Costantini, C., and Jaillon, S. (2011). Neutrophils in the activation and regulation of innate and adaptive immunity. Nat. Rev. Immunol. *11*, 519–531.
18. Zhang, Y., Zou, P., Gao, H., Yang, M., Yi, P., Gan, J., Shen, Y., Wang, W., Zhang, W., Li, J., et al. (2019). Neutrophil-lymphocyte ratio as an early new marker in AIV-H7N9-infected patients: a retrospective study. Ther. Clin. Risk Manag. *15*, 911–919.
19. Liu, J., Liu, Y., Xiang, P., Pu, L., Xiong, H., Li, C., Zhang, M., Tan, J., Xu, Y., Song, R., et al. (2020). Neutrophil-to-lymphocyte ratio predicts critical illness patients with 2019 coronavirus disease in the early stage. J. Transl. Med. *18*, 206.
20. Yan, X., Li, F., Wang, X., Yan, J., Zhu, F., Tang, S., Deng, Y., Wang, H., Chen, R., Yu, Z., et al. (2020). Neutrophil to lymphocyte ratio as prognostic and predictive factor in patients with coronavirus disease 2019: A retrospective cross-sectional study. J. Med. Virol. *92*, 2573–2581.
21. Daher, K.A., Selsted, M.E., and Lehrer, R.I. (1986). Direct inactivation of viruses by human granulocyte defensins. J. Virol. *60*, 1068–1074.
22. Okrent, D.G., Lichtenstein, A.K., and Ganz, T. (1990). Direct cytotoxicity of polymorphonuclear leukocyte granule proteins to human lung-derived cells and endothelial cells. Am. Rev. Respir. Dis. *141*, 179–185.
23. Currie, S.M., Findlay, E.G., McHugh, B.J., Mackellar, A., Man, T., Macmillan, D., Wang, H., Fitch, P.M., Schwarze, J., and Davidson, D.J. (2013). The human cathelicidin LL-37 has antiviral activity against respiratory syncytial virus. PLoS ONE *8*, e73659.
24. Gwyer Findlay, E., Currie, S.M., and Davidson, D.J. (2013). Cationic host defence peptides: potential as antiviral therapeutics. BioDrugs *27*, 479–493.
25. Klotman, M.E., and Chang, T.L. (2006). Defensins in innate antiviral immunity. Nat. Rev. Immunol. *6*, 447–456.
26. Tripathi, S., Tecle, T., Verma, A., Crouch, E., White, M., and Hartshorn, K.L. (2013). The human cathelicidin LL-37 inhibits influenza A viruses through a mechanism distinct from that of surfactant protein D or defensins. J. Gen. Virol. *94*, 40–49.
27. Malim, M.H., and Bieniasz, P.D. (2012). HIV Restriction Factors and Mechanisms of Evasion. Cold Spring Harb. Perspect. Med. *2*, a006940.

28. Jakobsen, M.R., Olagnier, D., and Hiscott, J. (2015). Innate immune sensing of HIV-1 infection. Curr. Opin. HIV AIDS *10*, 96–102.

29. Yin, X., Langer, S., Zhang, Z., Herbert, K.M., Yoh, S., König, R., and Chanda, S.K. (2020). Sensor Sensibility-HIV-1 and the Innate Immune Response. Cells *9*, 254.

30. Kourtis, A.P., Hudgens, M.G., and Kayira, D.; BAN Study Team (2012). Neutrophil count in African mothers and newborns and HIV transmission risk. N. Engl. J. Med. *367*, 2260–2262.

31. Ramsuran, V., Kulkarni, H., He, W., Mlisana, K., Wright, E.J., Werner, L., Castiblanco, J., Dhanda, R., Le, T., Dolan, M.J., et al. (2011). Duffy-null-associated low neutrophil counts influence HIV-1 susceptibility in high-risk South African black women. Clin. Infect. Dis. *52*, 1248–1256.

32. Cloke, T., Munder, M., Bergin, P., Herath, S., Modolell, M., Taylor, G., Müller, I., and Kropf, P. (2013). Phenotypic alteration of neutrophils in the blood of HIV seropositive patients. PLoS ONE *8*, e72034.

33. Salmen, S., Montes, H., Soyano, A., Hernández, D., and Berrueta, L. (2007). Mechanisms of neutrophil death in human immunodeficiency virus-infected patients: role of reactive oxygen species, caspases and map kinase pathways. Clin. Exp. Immunol. *150*, 539–545.

34. Butler, J.J., and Osborne, B.M. (1988). Lymph node enlargement in patients with unsuspected human immunodeficiency virus infections. Hum. Pathol. *19*, 849–854.

35. Klebanoff, S.J., and Coombs, R.W. (1992). Viricidal effect of polymorphonuclear leukocytes on human immunodeficiency virus-1. Role of the myeloperoxidase system. J. Clin. Invest. *89*, 2014–2017.

36. Saitoh, T., Komano, J., Saitoh, Y., Misawa, T., Takahama, M., Kozaki, T., Uehata, T., Iwasaki, H., Omori, H., Yamaoka, S., et al. (2012). Neutrophil extracellular traps mediate a host defense response to human immunodeficiency virus-1. Cell Host Microbe *12*, 109–116.

37. Barr, F.D., Ochsenbauer, C., Wira, C.R., and Rodriguez-Garcia, M. (2018). Neutrophil extracellular traps prevent HIV infection in the female genital tract. Mucosal Immunol. *11*, 1420–1428.

38. Yaseen, M.M., Abuharfeil, N.M., Yaseen, M.M., and Shabsoug, B.M. (2018). The role of polymorphonuclear neutrophils during HIV-1 infection. Arch. Virol. *163*, 1–21.

39. Imle, A., Kumberger, P., Schnellbächer, N.D., Fehr, J., Carrillo-Bustamante, P., Ales, J., Schmidt, P., Ritter, C., Godinez, W.J., Müller, B., et al. (2019). Experimental and computational analyses reveal that environmental restrictions shape HIV-1 spread in 3D cultures. Nat. Commun. *10*, 2144.

40. Ahmed, S.S., Bundgaard, N., Graw, F., and Fackler, O.T. (2020). Environmental Restrictions: A New Concept Governing HIV-1 Spread Emerging from Integrated Experimental-Computational Analysis of Tissue-Like 3D Cultures. Cells *9*, 1112.

41. Agosto, L.M., Uchil, P.D., and Mothes, W. (2015). HIV cell-to-cell transmission: effects on pathogenesis and antiretroviral therapy. Trends Microbiol. *23*, 289–295.

42. Glushakova, S., Baibakov, B., Margolis, L.B., and Zimmerberg, J. (1995). Infection of human tonsil histocultures: a model for HIV pathogenesis. Nat. Med. *1*, 1320–1322.

43. Grivel, J.C., and Margolis, L. (2009). Use of human tissue explants to study human infectious agents. Nat. Protoc. *4*, 256–269.

44. Penn, M.L., Grivel, J.C., Schramm, B., Goldsmith, M.A., and Margolis, L. (1999). CXCR4 utilization is sufficient to trigger CD4+ T cell depletion in HIV-1-infected human lymphoid tissue. Proc. Natl. Acad. Sci. USA *96*, 663–668.

45. Eckstein, D.A., Penn, M.L., Korin, Y.D., Scripture-Adams, D.D., Zack, J.A., Kreisberg, J.F., Roederer, M., Sherman, M.P., Chin, P.S., and Goldsmith, M.A. (2001). HIV-1 actively replicates in naive CD4(+) T cells residing within human lymphoid tissues. Immunity *15*, 671–682.

46. Homann, S., Tibroni, N., Baumann, I., Sertel, S., Keppler, O.T., and Fackler, O.T. (2009). Determinants in HIV-1 Nef for enhancement of virus replication and depletion of CD4+ T lymphocytes in human lymphoid tissue ex vivo. Retrovirology *6*, 6.

47. Fackler, O.T., Moris, A., Tibroni, N., Giese, S.I., Glass, B., Schwartz, O., and Kräusslich, H.G. (2006). Functional characterization of HIV-1 Nef mutants in the context of viral infection. Virology *351*, 322–339.

48. Wagar, L.E., Salahudeen, A., Constantz, C.M., Wendel, B.S., Lyons, M.M., Mallajosyula, V., Jatt, L.P., Adamska, J.Z., Blum, L.K., Gupta, N., et al. (2021). Modeling human adaptive immune responses with tonsil organoids. Nat. Med. *27*, 125–135.

49. Dancey, J.T., Deubelbeiss, K.A., Harker, L.A., and Finch, C.A. (1976). Neutrophil kinetics in man. J. Clin. Invest. *58*, 705–715.

50. Jayakumar, P., Berger, I., Autschbach, F., Weinstein, M., Funke, B., Verdin, E., Goldsmith, M.A., and Keppler, O.T. (2005). Tissue-resident macrophages are productively infected ex vivo by primary X4 isolates of human immunodeficiency virus type 1. J. Virol. *79*, 5220–5226.

51. Lämmermann, T., Bader, B.L., Monkley, S.J., Worbs, T., Wedlich-Söldner, R., Hirsch, K., Keller, M., Förster, R., Critchley, D.R., Fässler, R., and Sixt, M. (2008). Rapid leukocyte migration by integrin-independent flowing and squeezing. Nature *453*, 51–55.

52. Baldauf, H.M., Pan, X., Erikson, E., Schmidt, S., Daddacha, W., Burggraf, M., Schenkova, K., Ambiel, I., Wabnitz, G., Gramberg, T., et al. (2012). SAMHD1 restricts HIV-1 infection in resting CD4(+) T cells. Nat. Med. *18*, 1682–1687.

53. Chen, P., Hübner, W., Spinelli, M.A., and Chen, B.K. (2007). Predominant mode of human immunodeficiency virus transfer between T cells is mediated by sustained Env-dependent neutralization-resistant virological synapses. J. Virol. *81*, 12582–12595.

54. Sol-Foulon, N., Sourisseau, M., Porrot, F., Thoulouze, M.I., Trouillet, C., Nobile, C., Blanchet, F., di Bartolo, V., Noraz, N., Taylor, N., et al. (2007). ZAP-70 kinase regulates HIV cell-to-cell spread and virological synapse formation. EMBO J. *26*, 516–526.

55. Haller, C., and Fackler, O.T. (2008). HIV-1 at the immunological and T-lymphocytic virological synapse. Biol. Chem. *389*, 1253–1260.

56. Brinkmann, V., Reichard, U., Goosmann, C., Fauler, B., Uhlemann, Y., Weiss, D.S., Weinrauch, Y., and Zychlinsky, A. (2004). Neutrophil extracellular traps kill bacteria. Science *303*, 1532–1535.

57. Denk, S., Taylor, R.P., Wiegner, R., Cook, E.M., Lindorfer, M.A., Pfeiffer, K., Paschke, S., Eiseler, T., Weiss, M., Barth, E., et al. (2017). Complement C5a-Induced Changes in Neutrophil Morphology During Inflammation. Scand. J. Immunol. *86*, 143–155.

58. Haynes, D.R., Harkin, D.G., Bignold, L.P., Hutchens, M.J., Taylor, S.M., and Fairlie, D.P. (2000). Inhibition of C5a-induced neutrophil chemotaxis and macrophage cytokine production in vitro by a new C5a receptor antagonist. Biochem. Pharmacol. *60*, 729–733.

59. Monari, C., Kozel, T.R., Bistoni, F., and Vecchiarelli, A. (2002). Modulation of C5aR expression on human neutrophils by encapsulated and acapsular Cryptococcus neoformans. Infect. Immun. *70*, 3363–3370.

60. Woodfin, A., Voisin, M.B., and Nourshargh, S. (2010). Recent developments and complexities in neutrophil transmigration. Curr. Opin. Hematol. *17*, 9–17.

61. Phillipson, M., Heit, B., Colarusso, P., Liu, L., Ballantyne, C.M., and Kubes, P. (2006). Intraluminal crawling of neutrophils to emigration sites: a molecularly distinct process from adhesion in the recruitment cascade. J. Exp. Med. *203*, 2569–2575.

62. Pillay, J., Kamp, V.M., van Hoffen, E., Visser, T., Tak, T., Lammers, J.W., Ulfman, L.H., Leenen, L.P., Pickkers, P., and Koenderman, L. (2012). A subset of neutrophils in human systemic inflammation inhibits T cell responses through Mac-1. J. Clin. Invest. *122*, 327–336.

63. van Spriel, A.B., Leusen, J.H., van Egmond, M., Dijkman, H.B., Assmann, K.J., Mayadas, T.N., and van de Winkel, J.G. (2001). Mac-1 (CD11b/CD18) is essential for Fc receptor-mediated neutrophil cytotoxicity and immunologic synapse formation. Blood *97*, 2478–2486.

64. Gabali, A.M., Anzinger, J.J., Spear, G.T., and Thomas, L.L. (2004). Activation by inflammatory stimuli increases neutrophil binding of human immunodeficiency virus type 1 and subsequent infection of lymphocytes. J. Virol. *78*, 10833–10836.

65. Halle, S., Keyser, K.A., Stahl, F.R., Busche, A., Marquardt, A., Zheng, X., Galla, M., Heissmeyer, V., Heller, K., Boelter, J., et al. (2016). In Vivo Killing Capacity of Cytotoxic T Cells Is Limited and Involves Dynamic Interactions and T Cell Cooperativity. Immunity *44*, 233–245.

66. Orange, J.S. (2008). Formation and function of the lytic NK-cell immunological synapse. Nat. Rev. Immunol. *8*, 713–725.

67. Nandi, D., Gross, J.A., and Allison, J.P. (1994). CD28-mediated costimulation is necessary for optimal proliferation of murine NK cells. J. Immunol. *152*, 3361–3369.

68. Milligan, G.N. (1999). Neutrophils aid in protection of the vaginal mucosae of immune mice against challenge with herpes simplex virus type 2. J. Virol. *73*, 6380–6386.

69. Jan, M.S., Huang, Y.H., Shieh, B., Teng, R.H., Yan, Y.P., Lee, Y.T., Liao, K.K., and Li, C. (2006). CC chemokines induce neutrophils to chemotaxis, degranulation, and alpha-defensin release. J. Acquir. Immune Defic. Syndr. *41*, 6–16.

70. Keele, B.F., Giorgi, E.E., Salazar-Gonzalez, J.F., Decker, J.M., Pham, K.T., Salazar, M.G., Sun, C., Grayson, T., Wang, S., Li, H., et al. (2008). Identification and characterization of transmitted and early founder virus envelopes in primary HIV-1 infection. Proc. Natl. Acad. Sci. USA *105*, 7552–7557.

71. Salazar-Gonzalez, J.F., Bailes, E., Pham, K.T., Salazar, M.G., Guffey, M.B., Keele, B.F., Derdeyn, C.A., Farmer, P., Hunter, E., Allen, S., et al. (2008). Deciphering human immunodeficiency virus type 1 transmission and early envelope diversification by single-genome amplification and sequencing. J. Virol. *82*, 3952–3970.

72. Pear, W.S., Nolan, G.P., Scott, M.L., and Baltimore, D. (1993). Production of high-titer helper-free retroviruses by transient transfection. Proc. Natl. Acad. Sci. USA *90*, 8392–8396.

73. Platt, E.J., Wehrly, K., Kuhmann, S.E., Chesebro, B., and Kabat, D. (1998). Effects of CCR5 and CD4 cell surface concentrations on infections by macrophagetropic isolates of human immunodeficiency virus type 1. J. Virol. *72*, 2855–2864.

74. Vermeire, J., Roesch, F., Sauter, D., Rua, R., Hotter, D., Van Nuffel, A., Vanderstraeten, H., Naessens, E., Iannucci, V., Landi, A., et al. (2016). HIV Triggers a cGAS-Dependent, Vpu- and Vpr-Regulated Type I Interferon Response in $CD4^+$ T Cells. Cell Rep. *17*, 413–424.

75. Vladymyrov, M., Abe, J., Moalli, F., Stein, J.V., and Ariga, A. (2016). Real-time tissue offset correction system for intravital multiphoton microscopy. J. Immunol. Methods *438*, 35–41.

76. Ferrante, A., and Thong, Y.H. (1980). Optimal conditions for simultaneous purification of mononuclear and polymorphonuclear leucocytes from human blood by the Hypaque-Ficoll method. J. Immunol. Methods *36*, 109–117.

77. Wei, X., Decker, J.M., Liu, H., Zhang, Z., Arani, R.B., Kilby, J.M., Saag, M.S., Wu, X., Shaw, G.M., and Kappes, J.C. (2002). Emergence of resistant human immunodeficiency virus type 1 in patients receiving fusion inhibitor (T-20) monotherapy. Antimicrob. Agents Chemother. *46*, 1896–1905.

78. Ananth, S., Morath, K., Trautz, B., Tibroni, N., Shytaj, I.L., Obermaier, B., Stolp, B., Lusic, M., and Fackler, O.T. (2019). Multifunctional roles of the N-terminal region of HIV-1SF2Nef are mediated by three independent protein interaction sites. J. Virol. *94*, e01398-19.

79. Kaw, S., Ananth, S., Tsopoulidis, N., Morath, K., Coban, B.M., Hohenberger, R., Bulut, O.C., Klein, F., Stolp, B., and Fackler, O.T. (2020). HIV-1 infection of CD4 T cells impairs antigen-specific B cell function. EMBO J. *39*, e105594.

STAR★METHODS

KEY RESOURCE TABLE

REAGENT or RESOURCE	SOURCE	IDENTIFIER
Antibodies		
Brilliant Violet 785 (BV785) anti-human CD3 (clone UCHT1)	Biolegend	Cat#300472
Fluorescein isothiocyanate (FITC) anti-human CD66b (clone G10F5)	Biolegend	Cat#305104
Peridin-Chlorophyll-protein (PerCP) anti-human CD3 (clone SK7)	Biolegend	Cat#344814
Allophycocyanin (APC) anti-human CD8 (clone SK1)	Biolegend	Cat#344722
AlexaFluor® 700 anti-human CD18 (clone TS1/18)	Biolegend	Cat#302123
AlexaFluor® 594 anti-human CD11b (clone ICRF44)	Biolegend	Cat#301340
AlexaFluor® 647 anti-human CD11a (clone H111)	Biolegend	Cat#301218
Mouse anti-human MPO (clone 2C7)	Abcam	Cat#ab25989
AlexaFluor® 568 goat anti-mouse antibody	Life Technologies	Cat#A11004
Bacterial and virus strains		
HIV-$1_{NL4.3}$ SF2 Nef X4	Fackler et al.[47]	N/A
HIV-$1_{NL4.3}$ SF2 Nef R5	Fackler et al.[47]	N/A
T/F HIV-1 CH058	Keele et al.,[70] Salazar-Gonzalez et al.[71]	NIH AIDS Reagents
X4 HIV-1*GFP	Baldauf et al.[52]	N/A
Biological samples		
Human Peripheral Blood Mononuclear Cells from Buffy coats	Blood bank IKTZ Heidelberg	N/A
Polymorphonuclear neutrophils (PMNs) from human full blood	Blood donor volunters	N/A
Human tonsil tissue	Department of Otorhinolaryngology, Head and Neck Surgery, University Hospital Heidelberg, Germany	N/A
Chemicals, peptides, and recombinant proteins		
fixable viability dye eFluor™ 450	ebioscience	Cat#65-0863-18
DNase I, RNase free	Sigma-Aldrich	Cat#69182
Catalase	Sigma-Aldrich	Cat#C30-100MG
4-aminobenzoic acid hydrazide (4-ABAH)	Santa Cruz	Cat#sc204107
4-(2-aminoethyl) benzenesulfonylfluoride (AEBSF)	ThermoFisher	Cat#78431
iODN 2088	Enzo Life Sciences	Cat#ALX-746-250-T050
C5a Receptor Antagonist, W-54011 - CAS 405098-33-1	Calbiochem	Cat# 234415
N-Formylmethionine-leucyl-phenylalanine (fMLP)	Sigma-Aldrich	Cat#05-22-2500-25MG
PKH67	Sigma-Aldrich	Cat#MIDI67-1KT
Phorbol 12-myristate 13-acetate (PMA)	Sigma-Aldrich	Cat#P8139
fibronectin	Sigma-Aldrich	Cat#F4759-2MG
Hoechst 33342	Invitrogen	Cat#H3570
CellROX Oxidative Stress Reagent	ThermoFisher	Cat#C10444

(*Continued on next page*)

Continued

REAGENT or RESOURCE	SOURCE	IDENTIFIER
PKH26	Sigma Aldrich	Cat#MIDI26-1KT
Penicillin/Streptomycin Solution 100x	Capricorn	Cat#PS-B
DMEM, high glucose	GlutaMAX™ Supplement	Cat#61965026
Ficoll® Paque Plus	Merck	Cat# GE17144003
Critical commercial assays		
NETosis Assay Kit	Cayman	Cat#601010
Neutrophil MPO activity assay kit	Cayman	Cat#600620
Experimental models: cell lines		
Human embryonic kidney 293 T cells (HEK293T)	Pear et al.[72]	RRID:CVCL_1926; ATCC Cat#CRL-11268
TZM-bl cells, human carcinoma cell, derived from HeLa	NIH AIDS Reagents Program (Platt et al.[73])	PRID: CVCL_B478; Cat#8129-442
Oligonucleotides		
SG-PERT fwd primer; TCCTGCTCAACTTCCTGTCGAG	Vermeire et al.[74]	N/A
SG-PERT rev primer; CACAGGTCAAACCTCCTAGGAATG	Vermeire et al.[74]	N/A
Recombinant DNA		
pHIV-1NL4.3 SF2 Nef X4	Fackler et al.[47]	N/A
pHIV-1NL4.3 SF2 Nef R5	Fackler et al.[47]	N/A
pT/F HIV-1 CH058	Keele et al.,[70] Salazar-Gonzalez et al.[71]	NIH AIDS Reagents
X4 HIV-1* GFP	Baldauf et al.[52]	N/A
Software and algorithms		
BD FACSDiva Software	BD Biosciences	https://www.bdbiosciences.com/en-us
FlowJo software 10.4.2	BD Biosciences	https://www.flowjo.com/
Microsoft Office Excel 2016	Microsoft Office	https://www.microsoft.com/en-us/
Prism 6.0	GraphPad	https://www.graphpad.com:443/
BD FACSuite Software	BD Biosciences	https:www.bdbiosciences.com/en-us
ImSpector software	LaVision BioTec	https://www.lavisionbiotec.com/
Imaris software	Bitplane	https://imaris.oxinst.com/
Vivofollow software	Vladymyrov et al.[75]	N/A
Arivis Vision 4D	Arivis AG	https://www.arivis.com
InViewR	Arivis AG	https://www.arivis.com
Other		
Gelfoam® absorbable gelatin sponge 12cmx12cm	Pfizer	Cat# 59-9863
precision count beads	Biolegend	Cat#424902
Falcon® 96 Square Well Angled Bottom Insert Plate, with Lid, Sterile, 5/Case	Falcon	Cat#353938
Falcon® 96-well Multiwell Insert System with 1.0 μm Pore Translucent PET Membrane, with Feeder Tray and Lid, 1/ Case	Falcon	Cat#351130
Infinite 200 PRO plate reader	Tecan	N/A
Nikon Eclipse FN-1 upright microscope equipped with a 25X Nikon CFI-Apo (NA 1.1) objective	Nikon	N/A
TrimScope II 2PM system and Ti:Sapphire laser with an optical parametric oscillator (OPO, Coherent MPX Package)	LaVision Biotech	N/A
Fluorescence microscope IX81	Olympus	N/A

RESOURCE AVAILABILITY

Lead contact

Further information and requests for resources and reagents should be directed to and will be fulfilled by the Lead Contact, Prof. Dr. Oliver T. Fackler (oliver.fackler@med.uni-heidelberg.de).

Materials availability

There are no new materials generated in this paper. All material has to be requested from authors of cited references.

Data and code availability

Primary data from cytokine analysis generated in this study are available from the Lead Contact with a completed Material Transfer Agreement.

EXPERIMENTAL MODEL AND SUBJECT DETAILS

Human lymphoid aggregate culture (HLAC), human lymphoid histoculture (HLH) and peripheral blood mononuclear cells (PBMC)

HLACs and HLHs were generated as previously described.[42,43,46] Tonsils were removed and peripheral blood received from randomly selected anonymous donors with informed consent in accordance with the ethics vote S-123/2014 from the Heidelberg University Hospital ethics committee. Gender and age of the donors is not known. One half of each tonsil was collected during standard tonsillectomy while the other half was processed in the department of pathology to assess chronic tonsillitis and exclude any unexpected malignancy. Removed tonsil tissue was immediately transferred to 50ml Falcon tubes containing 1X phosphate-buffered saline (PBS) and either directly used for further processing or stored overnight at 4°C and processed the next day. Dead and burnt tissue was removed and tonsils were sliced into blocks of approximately 2mm size.

For the generation of HLAC tonsil tissue was mechanically disrupted and cells were filtered through a 40μm mash nylon strainer. The strainer was rinsed once with tonsil medium (RPMI 1640 GlutaMAX, 15% FCS, 5% Fungizone, 5% non-essential amino acids, 5% Gentamycin, 5% sodium pyruvate, 1% ampicillin) and cells were centrifuged at 1500rpm (Heraeus MEGAFUGE 40R) for 5min at room temperature. Cells were resuspended in 10ml of tonsil medium and viability and cell counts were determined by counting a 1:100 dilution with Trypan blue. Cells were resuspended in tonsil medium at $1x10^6$ cells/ml and 200μl of the cell suspension was added per well of a V bottom 96-well plate.

For culturing HLHs one Gelfoam® absorbable gelatin sponge (Pfizer) was cut into four equally sized pieces and each piece was added separately into one well of a 12-well plate. Each sponge was soaked with 500μl of tonsil medium and 4 tonsil blocks per sponge were placed on top. For culturing, additionally 1ml of tonsil medium was added. The HLAC and HLH were cultured at 37°C, 5% CO_2 under humidified conditions for up to three weeks.

Buffy coats for isolation of human PBMCs were obtained from healthy anonymous blood donors at the Heidelberg University Hospital Blood Bank according to the regulations of the local ethics committee. PBMC were isolated from buffy coats by Biocoll (Merck Biochrom) density gradient centrifugation using SepMate tubes (StemCell Technologies).

Isolation of polymorphonuclear neutrophils (PMN)

Heparinized blood from healthy volunteer donors (gender of the donors is not known), collected by venipuncture, was immediately used for PMN isolation as previously described with some modifications.[76] In brief, whole blood was diluted 1:2 in 1X PBS. 30ml of the blood-PBS mixture was overlaid on top of 15ml Biocoll Separating Solution (Merck) and centrifuged for 15min at 600 g without break at room temperature. The PMN layer on top of the red blood cells (RBCs) was collected and RBCs were removed by 2x hypotonic lysis with ice-cold water for 20sec. The lysis was stopped by the addition of 10X PBS. PMNs were either resuspended in tonsil medium or supplemented RPMI 1640 GlutaMAX (10% FCS, 5% Penicillin/Streptomycin). Viability and cell count after isolation were determined by counting a 1:10 dilution with Trypan blue. The purity of the isolated PMNs was always above 95%.

The viability of PMNs co-cultured with HLACs was determined by staining with fixable viability dye eFluor 450 (1:1000, ebioscience) for 20min in 1X PBS at 4°C. Cells were washed with 1X PBS before fixation with 3% paraformaldehyde (PFA) for 90min at room temperature. Cells were washed with 1X PBS and incubated with brilliant violet 785 (BV785)-conjugated antibodies against CD3 (1:100, clone UCHT1, Biolegend) and Fluorescein isothiocyanate (FITC)-conjugated antibodies against CD66b (1:100, clone G10F5, Biolegend) for 20min in 1X PBS. To determine absolute cell numbers 20μl of precision count beads (Biolegend) were added to 180μl of cells. Samples were measured by flow cytometry using a BD FACS Celesta with BD FacsDiva Software. Gating was done using FlowJo software 10.4.2 and data was processed with Microsoft Office Excel 2016 and GraphPad Prism 6.0 software.

Cell culture

Human embryonic kidney 293T (HEK293T) cells were cultured in Dulbecco's modified Eagle medium (DMEM; ThermoFisher Scientific) supplemented with FBS, 50 U/ml penicillin and 50 μg/ml streptomycin (Penicillin/Streptomycin Solution 100x Cat. No.PS-B, Firma Capricorn). The cells are female and have not been authenticated.

TZM-bl cells (also called JC53BL-13) were obtained from the NIH AIDS Research and Reference Reagent Program (Cat. no. 8129). The TZM-bl cell line is derived from a HeLa cell clone that was engineered to express CD4, CCR5 and CXCR4[73] and to contain integrated reporter genes for firefly Luc and *E. coli* β-galactosidase under the control of an HIV-1 long terminal repeat,[77] permitting sensitive and accurate measurements of infection.

METHOD DETAILS

Virus production, infectivity measurements, infection assays and CD4 T cell depletion

Virus production from 293T cells, infectivity measurements using SG-PERT for total viral particles and TZM-bl luciferase reporter assay were performed as described previously.[78] $2x10^6$ HLACs were infected with $1x10^{10}$ pU RT/well of the proviral CXCR4 tropic chimera HIV-1_{NL4-3} SF2 Nef WT (X4 HIV-1) in 200μl of tonsil medium. In some experiments, the proviral CCR5 tropic HIV-1_{NL4-3} SF2 Nef WT or the primary HIV-1 isolate transmission/founder virus (T/FV) CH058 were used for infection. For imaging experiments, HLHs were infected by the addition of $4x10^5$ infectious units X4 HIV-1*GFP (expresses GFP in productively infected cells[52]) per block in 6μl of tonsil medium. One day post-infection (dpi) HLACs were washed once with 200μl tonsil medium and HLHs were washed 3x with 1ml tonsil medium. $1x10^6$ freshly isolated PMNs were added to the HLAC or on top of the HLH. HLACs and HLHs were cultured for 11-14 days. Every two to three days supernatant for determination of viral titers was harvested and half of the medium was exchanged. The measurement started 1dpi with the initial supernatant collected after the washing step. To determine CD4 T cell depletion in HLACs, cells were harvested 11-14dpi, incubated with fixable viability dye eFluor 450 (1:1000, ebioscience) for 20min in 1X PBS. HLACs were washed with 1X PBS and incubated with Peridin-Chlorophyll-protein (PerCP)-conjugated antibodies against CD3 (1:100, clone SK7, Biolegend) and Allophycocyanin (APC)-conjugated antibodies against CD8 (1:100, clone SK1, Biolegend) for 20min in 1X PBS before fixation with 3% PFA for 90min. Samples were measured by flow cytometry using a BD FACSVerse with BD FACSuite Software. CD4 T cell depletion was quantified as described previously.[46] In brief, the CD4/CD8 ratio was calculated and the mean of the triplicate mock measurements was generated separately for mock – PMNs and mock + PMNs. The CD4/CD8 ratio of the infected samples -/+ PMNs was related to the respective $mock_{mean}$ -/+ PMNs. Gating was performed using FlowJo software 10.4.2 and data was processed with Microsoft Office Excel 2016 and GraphPad Prism 6.0 software.

Pharmacological inhibition of PMN effector functions

$2x10^6$ mock or X4 HIV-1 infected HLACs were co-cultured with $1x10^6$ PMNs in the presence of the indicated PMN inhibitors: 5U/ml rDNase I (Sigma-Aldrich), 1000U/ml Catalase (Sigma-Aldrich), 100μM 4-aminobenzoic acid hydrazide (4-ABAH; Santa Cruz), 50μM 4-(2-aminoethyl) benzenesulfonylfluoride (AEBSF; ThermoFisher), 1μM iODN 2088 (Enzo Life Sciences), and 300μM W-54011 (Merck). PMNs were pre-incubated with 100μg/ml blocking antibodies against CD18 (Clone TS1/18), CD11b (Clone ICRF44) and CD11a (Clone HI111) for 30min at room temperature. Viral titers were determined by SG-PERT similar to co-cultures in the absence of inhibitors.

1μm transwell assay

$1x10^6$ PMNs were resuspended in 260μl of tonsil medium and added per well of a 96 square well angled-bottom (Falcon). $2x10^6$ HLACs were resuspended in 70μl of tonsil medium and added per insert of a 96-well Insert System 1μm (Falcon). Every two to three days 5μl of supernatant were collected from the bottom well to determine the viral load via SG-PERT and half of the medium was exchanged. The measurement started 1dpi with the initial supernatant collected after the washing step.

3μm transwell chemotaxis assay

A 96-well transwell system with 3μm pore size was coated with 2.5μg/ml fibronectin for 1h at 37°C. 200μl of tonsil medium containing either medium alone, DMSO, 100nM N-Formylmethionine-leucyl-phenylalanine (fMLP) or $2x10^6$ mock or infected HLACs or PBMCs were added to the bottom well. The insert was placed into the bottom well and 60μl tonsil medium containing $3x10^4$ PMNs labeled with PKH67 (Sigma-Aldrich), according to manufacturer's instructions, were added into the insert. Cells were allowed to migrate for 3 h and 24h at 37°C. 50mM EDTA were added to the bottom well and incubated for 10min at 4°C. Cells within the bottom well were collected, resuspended in 200μl 1X PBS containing 20μl precision counting beads (Biolegend) and the amount of migrated PMNs was analyzed by flow cytometry (BD FACS Verse). The number of events in the FITC positive population and the number of counting beads was quantified and absolute PMN counts were calculated.

Supernatant swap experiment

$2x10^6$ X4 HIV-1 infected HLACs were co-cultured with $1x10^6$ PMNs for 3, 6, 24, 48 and 72h. Co-culture supernatant was transferred after the indicated time points to X4 HIV-1 infected HLACs only. Every two to three days 5μl of supernatant were collected to determine the viral load via SG-PERT and half of the medium was exchanged. The measurement started 1dpi with the initial supernatant collected after the washing step.

Neutrophil elastase (NE) activity

$2x10^6$ mock or X4 HIV-1 infected HLACs were co-cultured with $1x10^6$ PMNs for 3 and 24h. Mock HLACs co-cultured with PMNs in the presence of PMA (20nM, Sigma-Aldrich) served as a positive control. NE activity was analyzed by the NETosis Assay Kit (Cayman)

according to the manufacturer's instructions. In brief, after the indicated incubation time the supernatant was aspirated and the cells were washed twice by the addition of 200µl prewarmed NET Assay Buffer followed by the addition of 200µl S7 Nuclease for 15min at 37°C. 200µl of the supernatant was transferred to a 96-well flat bottom plate containing 4µl of EDTA Assay Reagent solution and centrifuged for 5min at 300 g. To inactivate HIV-1, 180µl of the supernatant was transferred to a new 96-well flat bottom plate containing 20µl of 5% Triton X-100 and incubated for 10min at room temperature. For the preparation of the assay, 100µl of standard and sample were added to a new 96-well flat bottom plate, 100µl of the 1:30 diluted Elastase substrate was added, the plate was covered and incubated for 1-2h at 37°C. The cover was removed and the absorbance was analyzed at 405nm using the Infinite 200 PRO plate reader (Tecan).

Neutrophil MPO activity assay kit

$1x10^6$ PMNs were incubated in the presence or absence of 20nm PMA for 3h and cells were analyzed according to the manufacturer's instructions (Cayman, 600620). Briefly, 25µl of the supernatant were transferred to a 96-well flat bottom plate and either incubated with the same amount of assay buffer or Cell-Based Assay MPO Inhibitor solution. The 3,3¿,5,5¿-tetramethyl-benzidine (TMB) substrate solution was added and the plate was incubated for 10min at room temperature before reading the absorbance at 650nm with a Tecan plate reader.

Immunofluorescence

NET formation was monitored by the presence of extracellular DNA covered with MPO. Cover glasses (CS) were coated with fibronectin (2.5µg/ml, Sigma-Aldrich) for 1h. $3x10^4$ freshly isolated PMNs were resuspended in 30µl of RPMIΔ (RPMI 1640 GlutaMAX without supplements), seeded on CS and allowed to adhere for 20min. 20µl of medium containing either medium alone, DMSO, 100nM PMA or different amounts of HIV-1 viral particles were added to the CS and cells were incubated for 3 or 24h at 37°C, 5% CO_2. Cells were then fixed with 3% PFA for 90min at room temperature, permeabilized with 0.1% Triton X-100 and stained with anti-human MPO (1:100, clone 2C7, Abcam) followed by Alexa Fluor 568 goat anti-mouse antibody (1:2000, Life Technologies). Cells were additionally stained with Hoechst 33342 (1:10000, Invitrogen).

Quantification of NET formation was performed as follows: 5 random sections on the CS were imaged. Cells were divided in three categories: lobular nucleus, round nucleus and NET forming cell. The cells were attributed to one of the categories, counted manually and the percentage was calculated. NET formation in PMA treated samples was artificially set to 100% since the entire CS was covered with NETs which did not allow distinction.

Reactive oxygen species (ROS) production

$2x10^6$ mock or X4 HIV-1 infected HLACs were co-cultured with $1x10^6$ PMNs for 3 and 24h. Mock HLACs co-cultured with PMNs in the presence of PMA (20nM) served as a positive control. ROS production was analyzed using CellROX Oxidative Stress Reagent (ThermoFisher) according to the manufacturer's instructions. In brief, after the indicated incubation time cells were washed once with 1X PBS and incubated with 5µM of CellROX oxidative stress reagent for 30min at 37°C. Cells were washed with 1X PBS and fixed with 3% PFA for 90min. After washing once with 1X PBS the cells were resuspended in 200µl of 1X PBS and measured using a BD FACS Verse or BD FACS Celesta with BD FACSuite or FacsDiva Software, respectively. The gating strategy was as follows. PMNs and HLACs were separated via FSC and SSC (PMNs = SSC_{high}, FSC_{high}) and the median fluorescence intensity (MFI) of the FITC signal within the PMN population was measured.

2-photon microscopy (2PM) of HLHs

HLHs were infected or not with $4x10^5$ infectious units HIV-1* GFP. Three dpi HLH was transferred into a grease-sealed silicone ring on a pre-warmed metal plate, filled with conditioned tonsil medium containing 20mM HEPES. $1x10^6$ freshly isolated PMNs, labeled with PKH26 (Sigma Aldrich) according to manufacturer's instructions, were added on top of the tissue block and the block was sealed with a cover glass. Imaging was performed immediately or 3h after PMN addition using a Nikon Eclipse FN-1 upright microscope equipped with a 25X Nikon CFI-Apo (NA 1.1) objective and a TrimScope II 2PM system controlled by ImSpector software (LaVision BioTec) combined with an automated system for real-time correction of tissue drift.[75] For 2-photon excitation, a Ti:Sapphire laser with an optical parametric oscillator (OPO, Coherent MPX Package) were tuned to 880nm and 1200nm, respectively. For 4-dimensional analysis of cell migration, 16 x-y sections with z-spacing of 2µm (30µm depth) were acquired every 20sec for up to 3h; the field of view was up to 400x400µm. Emitted light and second harmonic signals were detected through 447/60-nm, 525/50-nm, 595/50-nm and 690/50-nm bandpass filters using non-descanned detectors. Time-lapse movies were reconstructed and analyzed using Arivis Vision4D software (Arivis AG) and interactions of PMNs with HIV infected GFP positive lymphocytes were manually tracked by InViewR (Arivis AG) as published previously.[79]

QUANTIFICATION AND STATISTICAL ANALYSIS

Statistical analysis of datasets was carried out using Prism version 6.0 (GraphPad). Statistical significance was calculated using the Mann-Whitney U test. n.s., not significant; *, $p < 0.05$; **, $p < 0.01$; ****, $p < 0.0001$. See figure legends for details.